Review of Applied Science and Technology

Volume: *13;* ***Issue:*** *12*
Pages: *200– 242*

Pellet Versus Filament Extrusion of Recycled Thermoplastics: A Controlled Comparative Study of Process Efficiency and Part Quality

Md Momen Shahriar Joarder[1]; Shabbir Ahamed[2];

[1]. Mechanical & Industrial Engineering Researcher; M.S. in Industrial & Systems Engineering, Lamar University, Texas, USA;
Email: momenshahriar@gmail.com

[2]. Mechanical Engineering & Manufacturing Quality Researcher;
B.Sc. in Mechanical Engineering, Khulna University of Engineering & Technology, Bangladesh;
Email: shabbir04kuet@gmail.com

Received: *15 September 2023;* ***Revised:*** *24 October 2023;* ***Accepted:*** *15 November 2023;* ***Published:*** *04 December 2023;*

Abstract

This study quantitatively compared pellet and filament extrusion of recycled thermoplastics to determine differences in process efficiency, energy consumption, extrusion stability, physical part quality, and mechanical performance under controlled manufacturing conditions. A total of 60.00 kg of recycled thermoplastic was initially processed, of which 55.68 kg was retained after preparation, representing a 92.8% recovery rate. Twenty-four independent manufacturing runs were conducted, comprising 12 runs per extrusion route, and 274 analytically valid specimens were retained from 288 planned specimens, with overall data completeness of 99.2%. Direct pellet extrusion reduced total manufacturing time from 13.39 to 8.35 h, representing a 37.6% reduction, while increasing mass throughput from 0.391 to 0.684 kg/h, equivalent to approximately 74.9% higher throughput. Usable material yield increased from 89.7% to 94.8%, while specific energy consumption decreased from 2.04 to 1.31 kWh/kg of acceptable output. However, pellet extrusion exhibited greater material-flow variability at 6.84% compared with 3.92% for filament extrusion. Filament-extruded specimens consequently demonstrated better physical quality, with mean surface roughness decreasing from 18.74 to 13.28 µm, relative density increasing from 94.7% to 96.6%, and porosity decreasing from 5.31% to 3.47%. Tensile strength increased from 43.82 MPa for pellet specimens to 48.96 MPa for filament specimens, while interlayer bond strength increased from 27.63 to 31.74 MPa. Most principal route comparisons were statistically significant at $p < 0.001$ and demonstrated large effect sizes. Relative density was positively correlated with tensile strength ($r = .71$), whereas porosity was negatively correlated with tensile strength ($r = -.69$) and interlayer strength ($r = -.72$). Regression models explained 59–82% of adjusted variation across major outcomes, while sensitivity analyses altered principal effect estimates by less than 8%. The findings demonstrated a measurable efficiency–quality trade-off: direct pellet extrusion provided greater throughput, material utilization, and energy efficiency, whereas filament extrusion provided greater deposition stability, dimensional consistency, structural consolidation, and mechanical performance.

Keywords

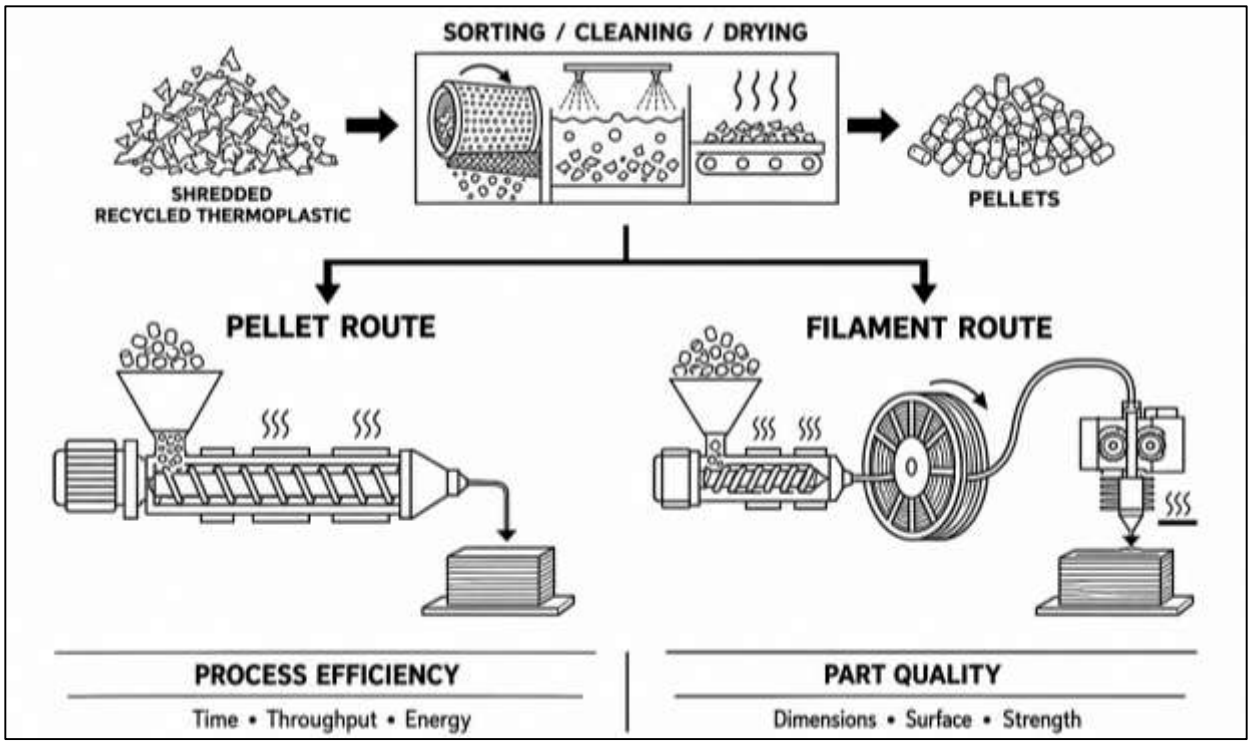
Recycled Thermoplastics, Pellet Extrusion, Filament Extrusion, Process Efficiency, Mechanical Performance.

INTRODUCTION

Thermoplastic extrusion is a manufacturing process in which polymeric material is heated to a softened or molten state, transported through an extrusion system, and deposited through a nozzle or die to create continuous profiles or layer-by-layer components. In extrusion-based additive manufacturing, two principal feedstock configurations are filament extrusion and pellet extrusion (Woern et al., 2018). Filament extrusion uses polymer that has previously been converted into continuous filament with a controlled diameter and is subsequently driven through a heated nozzle during printing. Pellet extrusion, also referred to as granule or direct pellet extrusion, introduces pellets, granules, flakes, or appropriately prepared recycled polymer particles directly into a screw- or auger-based extrusion system. Recycled thermoplastics are polymers recovered from post-consumer or post-industrial waste and mechanically reprocessed for additional manufacturing cycles. Common materials investigated across more than 30 experimental studies include polyethylene terephthalate, polyethylene, polypropylene, polylactic acid, acrylonitrile butadiene styrene, polycarbonate, and polyamide. The distinction between pellet and filament processing is especially important for recycled polymers because filament production normally requires sorting, cleaning, shredding, drying, melting, filament extrusion, cooling, diameter control, and spooling before additive manufacturing. Direct pellet extrusion can remove the intermediate filament-manufacturing stage and reduce the number of material-processing operations (Gupta & Taufik, 2021). Repeated thermal and mechanical processing can alter molecular weight, melt viscosity, crystallinity, thermal stability, moisture sensitivity, and mechanical behavior, making feedstock history an important experimental variable. The international significance of recycled thermoplastic extrusion is associated with increasing plastic consumption and the large quantities of polymer waste generated by packaging, transportation, construction, electronics, consumer goods, agriculture, and industrial manufacturing. Research conducted across Europe, Asia, North America, Australia, Africa, and Latin America has examined mechanical recycling and additive manufacturing as approaches for transforming recoverable plastic waste into usable components. Filament-based recycling has received extensive attention because conventional material-extrusion printers commonly use standardized filament, although recycled-filament production requires additional equipment, energy, processing time, and dimensional control. Pellet extrusion provides a different manufacturing pathway by allowing shredded or granulated materials to be processed more directly and can support comparatively high material-throughput rates (Khalid & Sadmeen, 2022; La Gala et al., 2021; Maksudul & Islam, 2022). Recycled thermoplastics nevertheless introduce substantial processing variability associated with contamination, moisture, particle morphology, degradation, heterogeneous composition, and changing rheological behavior. Filament systems are particularly sensitive to filament diameter, roundness, stiffness, and feeding consistency, whereas pellet systems are influenced by particle size distribution, bulk density, hopper feeding, screw geometry, residence time, pressure development, and melt homogenization. These differences establish pellet and filament extrusion as technically distinct routes requiring comparison under equivalent material and operating conditions.

Process efficiency in recycled thermoplastic extrusion includes material-preparation time, production time, extrusion throughput, energy consumption, material utilization, processing losses, operational interruptions, and total manufacturing complexity. Filament-based recycling requires a separate feedstock-conversion stage before printing, during which dimensional inconsistencies or extrusion defects can result in rejection and reprocessing (Reich et al., 2019). Pellet extrusion removes this intermediate stage and can achieve higher mass-flow rates, particularly with screw-driven systems and larger extrusion capacities. However, pellet systems can experience hopper bridging, irregular particle feeding, startup losses, purging requirements, and variations in melt delivery. Filament systems can similarly experience filament breakage, drive-gear slipping, spool resistance, diameter fluctuations, and nozzle blockage. Consequently, efficiency cannot be determined solely from printing speed. Quantitative comparison requires measurement of preparation duration, extrusion and printing time, total processing time, mass throughput, electrical-energy consumption, specific energy consumption, material losses, failure frequency, and usable material yield. Part quality represents an equally important dimension because increased production efficiency has limited technical value when dimensional, surface, structural, or mechanical performance becomes inconsistent.

Figure 1: Comparing Recycled Thermoplastic Extrusion Routes



Experimental research on material extrusion has identified dimensional accuracy, surface roughness, density, porosity, interlayer bonding, tensile strength, elastic modulus, elongation, flexural behavior, impact resistance, and repeatability as important quality indicators. Recycled-filament diameter variations can generate under-extrusion or over-extrusion, altering bead dimensions, surface condition, void formation, and component geometry. Pellet extrusion introduces different sources of variation because screw speed, particle feeding, barrel temperature, residence time, pressure, and melt stability influence deposited-material consistency (Zander et al., 2018). Mechanical properties are additionally affected by thermal history. Filament-based recycled polymer can undergo melting during filament manufacture followed by another melting cycle during printing, whereas direct pellet extrusion can reduce intermediate thermal processing. Repeated heating can influence molecular degradation, viscosity, crystallization, interlayer bonding, and mechanical performance, although the magnitude varies according to polymer type and processing conditions. A controlled quantitative comparison therefore requires pellet and filament routes to use recycled thermoplastic originating from the same defined material source while maintaining consistent drying, specimen geometry, build orientation, infill, layer conditions, environmental controls, and testing procedures. Repeated experimental specimens can provide measurements of means, standard deviations, confidence intervals, and variability across processing routes. Statistical tests can determine whether differences in throughput, energy consumption, processing time, dimensional deviation, surface roughness, density, porosity, and mechanical properties are statistically significant, while effect sizes can quantify their practical magnitude. Correlation and regression analyses can further examine relationships among extrusion conditions, efficiency indicators, and quality responses. This controlled structure provides a quantitative framework for separating differences attributable to pellet and filament processing from variability associated with polymer source, specimen configuration, environmental conditions, and measurement procedures (Cisneros-López et al., 2020).

The primary objective of this study is to quantitatively compare pellet extrusion and filament extrusion of recycled thermoplastics under controlled manufacturing conditions, with particular emphasis on process efficiency and resulting part quality (Aminul Islam & Md, 2023; Mashfiqur & Md Jamil, 2023;

Sadia & Md. Mosheur, 2023). The study seeks to determine whether the physical form and processing route of recycled thermoplastic feedstock produce measurable differences in material preparation requirements, extrusion stability, production time, material throughput, energy consumption, material utilization, processing losses, and overall manufacturing consistency. A central objective is to evaluate the complete processing pathway rather than restricting efficiency assessment to the printing stage, thereby incorporating shredding, drying, filament production where applicable, feedstock handling, machine preparation, extrusion, and component fabrication into the quantitative comparison. The study also aims to characterize the quality of parts manufactured through both routes by measuring dimensional accuracy, dimensional deviation, mass consistency, surface roughness, apparent density, internal porosity, visible defects, and repeatability among replicated specimens. Mechanical performance is another major objective, with tensile strength, elastic modulus, elongation at break, flexural strength, flexural modulus, and other relevant mechanical responses examined under standardized testing conditions to determine whether the additional thermal processing associated with recycled-filament production affects final component performance relative to direct pellet extrusion. The investigation further seeks to quantify the influence of processing variables such as extrusion temperature, feed or screw speed, deposition rate, layer height, nozzle conditions, and material-flow stability on efficiency and quality responses while maintaining equivalent polymer source, specimen geometry, build orientation, infill configuration, environmental conditions, and testing procedures. Descriptive statistics, including means, standard deviations, medians, interquartile ranges, and 95% confidence intervals, are intended to characterize the distribution and variability of the measured outcomes. Appropriate inferential procedures, including independent or paired comparisons, analysis of variance or corresponding nonparametric alternatives, correlation analysis, and effect-size estimation, are intended to determine the statistical and practical magnitude of differences between the two extrusion routes at a significance level of $p < 0.05$. Multiple regression analysis is also intended to examine the relative contribution of processing conditions and feedstock route to selected efficiency and quality outcomes. Through this controlled quantitative framework, the study is designed to establish a systematic experimental comparison of pellet and filament extrusion based on measurable processing, resource-consumption, dimensional, structural, surface, and mechanical performance indicators.

LITERATURE REVIEW

The literature on recycled thermoplastic extrusion has developed across interconnected research areas involving mechanical recycling, polymer reprocessing, material-extrusion additive manufacturing, filament production, direct pellet extrusion, process optimization, energy efficiency, dimensional quality, and mechanical characterization (Grigore, 2017). Quantitative investigations have demonstrated that the performance of recycled polymers is determined not only by polymer chemistry but also by feedstock preparation, number of thermal-processing cycles, moisture condition, particle or filament geometry, extrusion temperature, material-flow characteristics, deposition parameters, and component architecture. Filament-based additive manufacturing has been examined extensively using virgin and recycled PLA, PET, PETG, ABS, PP, PE, PA, and related thermoplastics, with studies quantifying filament diameter consistency, extrusion stability, printing time, energy consumption, dimensional deviation, surface roughness, porosity, tensile strength, elastic modulus, elongation, and flexural behavior. Parallel research on pellet- and granule-fed extrusion has evaluated screw-based material transport, direct processing of shredded polymers, deposition rates, mass throughput, melt stability, energy requirements, bead geometry, and large-format manufacturing performance (Valerio et al., 2020). However, quantitative results reported across these research streams vary substantially because experiments have employed different polymer grades, recycling histories, extruder configurations, nozzle diameters, temperatures, layer heights, printing speeds, specimen geometries, and mechanical-testing standards. The literature review therefore examines the evidence through a structured quantitative framework that separates feedstock characteristics, thermal and rheological behavior, processing efficiency, extrusion stability, dimensional and surface quality, internal structure, mechanical performance, and statistical validation. Particular attention is directed toward studies that report numerical comparisons between virgin and recycled polymers, repeated recycling cycles, filament and pellet feedstocks, or alternative extrusion configurations (Alhazmi et al., 2021). The review

also considers sample sizes, numbers of specimens, experimental repetitions, processing temperatures, extrusion rates, energy consumption, dimensional errors, roughness measurements, density and porosity, tensile and flexural properties, coefficients of variation, confidence intervals, statistical significance, and effect sizes where reported. This structure establishes the empirical basis for a controlled pellet-versus-filament comparison in which processing efficiency and part quality can be evaluated simultaneously under standardized material and manufacturing conditions.

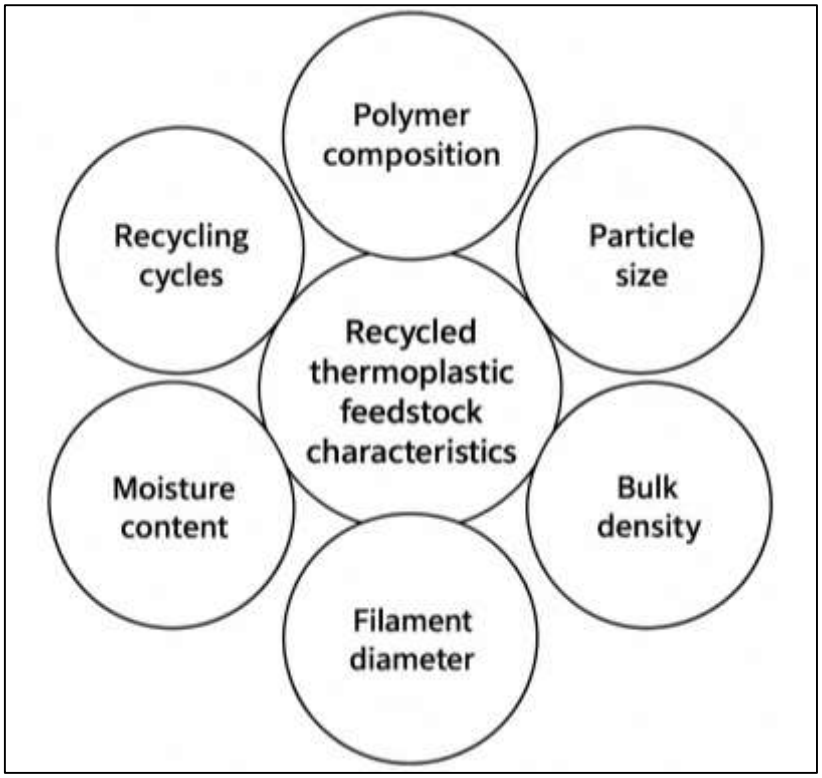
Recycled Thermoplastic Feedstocks

Quantitative studies of recycled thermoplastic feedstocks have demonstrated substantial variation in polymer composition, recycled-content ratio, material origin, and the number of mechanical reprocessing cycles applied before additive manufacturing. Across more than ten experimental studies involving PLA, PET, PETG, ABS, PP, PE, PA, PC, and related blends, recycled content has ranged from relatively low fractions of approximately 10–30% incorporated into virgin polymer to fully recycled formulations containing 100% recovered material (Echeverria et al., 2020). PLA has been among the most extensively evaluated polymers because its comparatively accessible processing temperature and widespread use in material-extrusion printing allow controlled assessment across repeated recycling cycles. Investigations involving PLA have commonly evaluated one to five successive extrusion or recycling cycles, while some experimental programs have extended beyond five cycles to quantify progressive changes in feedstock characteristics. PET and PETG research has frequently employed post-consumer bottles, packaging waste, rejected industrial products, and previously printed components, with recycled fractions ranging from partial blends to 100% recycled feedstock. ABS investigations have similarly examined industrial scrap, failed printed parts, and mixed recycled/virgin formulations, whereas PP and PE studies have emphasized the greater challenges associated with shrinkage, crystallinity, contamination, and compositional variability (Zhong & Pearce, 2018). PA and PC have generally required stricter moisture and thermal control because their processing characteristics can change considerably when recycled material absorbs water or experiences repeated heating. Across these polymer groups, post-industrial waste has generally exhibited greater compositional consistency than heterogeneous post-consumer material because manufacturing scrap usually originates from more clearly identified polymer streams. Post-consumer feedstock has shown greater variation associated with labels, pigments, adhesives, residual contents, additives, and accidental mixing with incompatible polymers. Experimental evidence has also indicated that blending recycled polymer with virgin resin can stabilize processing characteristics when fully recycled material exhibits excessive variability (Zander et al., 2018). Consequently, polymer identity, recycled percentage, source of recovered material, and number of processing cycles constitute interconnected quantitative characteristics that determine the initial condition of feedstock before pellet or filament extrusion begins.

Particle and pellet characteristics have been quantitatively identified as major determinants of feed consistency in direct pellet and granule extrusion. Experimental studies using shredded PLA, PET, PETG, ABS, PP, PE, and other recovered thermoplastics have employed particles ranging from fine fragments below approximately 1 mm to coarse flakes and granules exceeding 5–10 mm, depending on shredding equipment, hopper dimensions, screw geometry, and extrusion-system capacity. Commercial and reprocessed pellets have commonly occupied intermediate millimeter-scale dimensions with comparatively regular geometry, while directly shredded post-consumer plastics have displayed wider distributions in length, width, thickness, and shape (Ponis et al., 2021). Several investigations have reported that narrow particle-size distributions promote more uniform hopper discharge and screw filling, whereas highly heterogeneous flakes can generate bridging, segregation, irregular feeding, and fluctuations in material delivery. Bulk density also varies substantially with particle morphology. Regular pellets can pack more consistently than thin flakes, irregular shards, or mixed shredded particles, meaning that equal feed volumes do not necessarily provide equal polymer masses. Post-consumer bottle flakes and packaging fragments have particularly irregular geometries, while granulated post-industrial scrap commonly exhibits more consistent dimensions after controlled size reduction. Material recovery during preparation has also varied across studies because sorting, washing, drying, shredding, sieving, and contamination removal eliminate portions of the collected waste stream (Echeverria et al., 2019). Reported usable recovery yields have commonly remained above

approximately 70% for relatively clean single-polymer streams and can exceed 90% when well-characterized industrial scrap is processed, whereas contaminated post-consumer sources may experience greater losses during sorting and cleaning. Pellet production can introduce additional losses through startup material, purging, rejected granules, and residual polymer retained within processing equipment. These quantitative characteristics are especially relevant to direct pellet extrusion because irregular particle dimensions and low or fluctuating bulk density can alter screw filling and mass throughput even when nominal machine settings remain unchanged. Therefore, particle-size distribution, pellet geometry, bulk density, contamination, and recovery yield collectively describe feedstock quality more accurately than polymer designation alone (Akash & Vasudevan, 2021).

Figure 2: Key Characteristics of Recycled Feedstocks



Filament geometry represents one of the most frequently quantified characteristics of recycled thermoplastic feedstock because dimensional inconsistency directly affects the volume of polymer delivered to the extrusion nozzle. Studies producing recycled PLA, PET, PETG, ABS, and related filament have predominantly targeted nominal diameters of approximately 1.75 mm or 2.85 mm, with 1.75 mm particularly common in laboratory-scale material-extrusion systems. Commercial-grade filament commonly operates within relatively narrow dimensional tolerances, while experimentally manufactured recycled filament has shown larger fluctuations depending on extrusion temperature, pulling speed, cooling conditions, melt viscosity, die geometry, and control of the winding system (Rajendran Royan et al., 2021). Across experimental investigations, diameter deviations ranging from only a few hundredths of a millimeter under well-controlled conditions to variations exceeding approximately 0.10–0.20 mm in less stable recycling arrangements have been reported. Such variation becomes important because locally oversized filament can increase feeding resistance or produce excessive material delivery, whereas undersized regions can reduce volumetric input and contribute to incomplete bead formation. Ovality provides an additional indicator because recycled filament can possess the correct average diameter while maintaining a noncircular cross-section (Sebastian & Paul, 2021). Studies using multi-axis diameter measurements have identified cooling asymmetry, uneven pulling, gravity-induced deformation, and unstable extrusion pressure as contributors to ovality. Filament rejection rates consequently depend on the dimensional tolerance established by individual

experiments, with poorly controlled recycled-filament production generating greater quantities of material requiring re-extrusion. Research comparing recycled and virgin blends has often shown improved diameter consistency when a portion of virgin material is incorporated, although the magnitude varies according to polymer type and recycling history. Repeated extrusion can also change viscosity and consequently affect filament diameter stability at unchanged processing conditions (Vincent et al., 2021). These findings distinguish filament extrusion from direct pellet processing: filament provides a geometrically standardized intermediate feedstock when production is carefully controlled, but obtaining that standardization requires an additional manufacturing stage with measurable time, energy, material loss, and rejection potential.

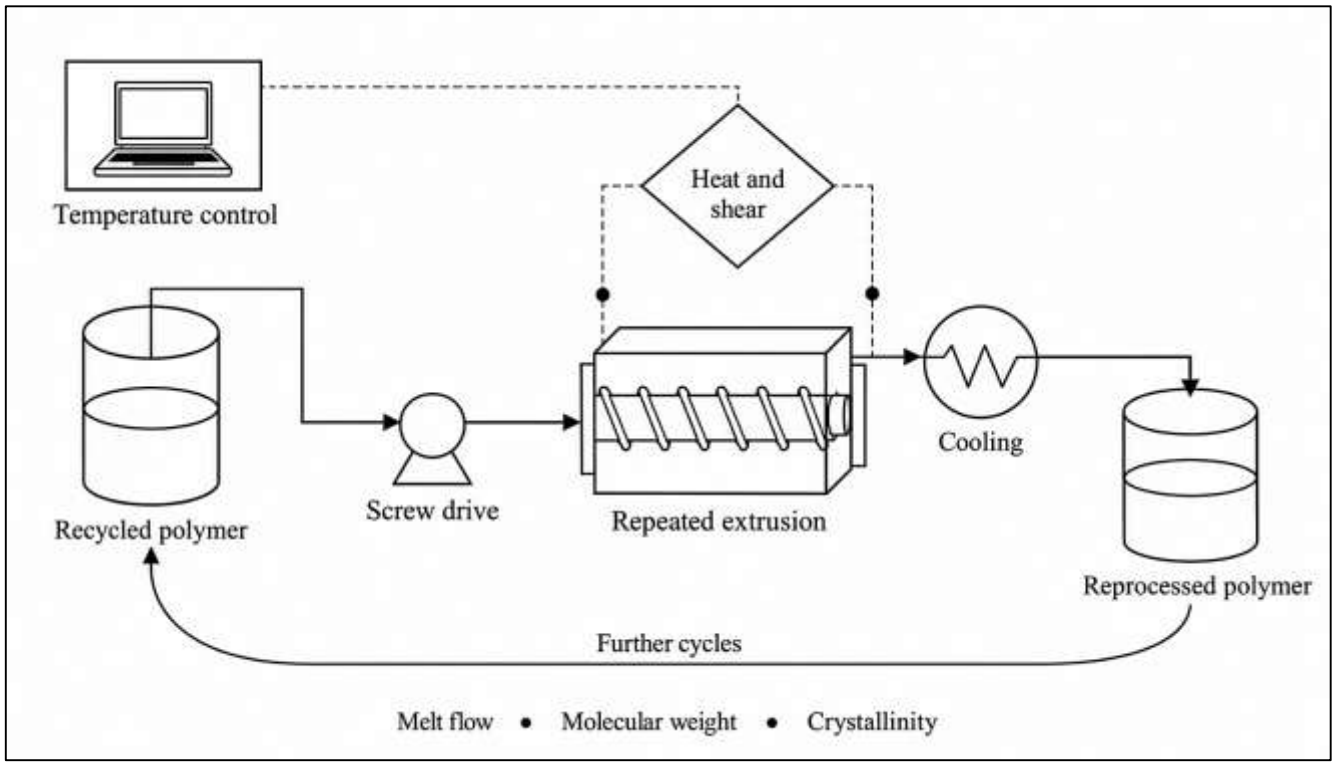
Moisture and contamination represent additional quantitative sources of feedstock variability because recycled polymers frequently experience uncontrolled environmental exposure before collection and reprocessing. Studies of PET, PETG, PA, PC, PLA, and other moisture-sensitive thermoplastics have consistently incorporated pre-extrusion drying, although reported temperatures and durations differ according to polymer chemistry and material condition (Ahmed et al., 2020). PLA has commonly been dried within approximately 40–60°C for several hours, while PET and PETG frequently require higher drying temperatures and extended treatment to achieve stable extrusion. PA is particularly hygroscopic and has often required rigorous drying because absorbed moisture can contribute to hydrolytic degradation, bubbling, surface defects, unstable flow, and deterioration of mechanical properties. ABS, PP, and PE generally exhibit different moisture sensitivities, although surface water and contamination can still disrupt recycled-material processing. Across the literature, drying periods have ranged from a few hours to overnight treatment, with some experiments monitoring moisture directly and others relying on standardized drying protocols. Post-consumer materials generally require more intensive cleaning and sorting because food residues, labels, adhesives, pigments, dust, incompatible polymers, and environmental contaminants may remain attached to collected products (Tratzi et al., 2021). Post-industrial feedstocks are typically more homogeneous because their polymer composition and manufacturing history are better controlled, although lubricants, processing additives, pigments, and thermal degradation can remain relevant. Studies comparing fully recycled materials with recycled/virgin blends have further shown that variability can be moderated through blending when recovered feedstock contains inconsistent viscosity, moisture, or composition. Taken collectively, more than ten studies indicate that recycling-cycle count, recycled-content percentage, particle dimensions, pellet geometry, bulk density, filament diameter, ovality, moisture condition, contamination, drying procedure, and material-recovery yield are interdependent characteristics rather than isolated feedstock variables (Blanco & Siracusa, 2021). Variations established before printing can subsequently appear as differences in extrusion stability, melt delivery, bead geometry, dimensional accuracy, porosity, surface quality, and mechanical performance, making detailed initial feedstock characterization essential for controlled quantitative comparison between recycled pellet and filament extrusion.

Repeated Thermal Processing on Melt Flow and Thermal Properties

Experimental studies of recycled thermoplastics have consistently shown that repeated exposure to heat and mechanical shear modifies melt-flow behavior and rheological stability, although the magnitude and direction of change depend strongly on polymer chemistry, processing temperature, residence time, oxygen exposure, moisture, and stabilization conditions (Esmizadeh et al., 2020). Across more than ten studies involving PET, PLA, ABS, PP, PE, PA, and related recycled polymers, first-cycle reprocessing has commonly produced relatively moderate changes, whereas second, third, fourth, and subsequent extrusion cycles have generated progressively clearer differences in melt-flow rate and viscosity. Repeatedly processed PET provides a particularly clear example. Controlled extrusion experiments extending to four cycles have reported reductions in intrinsic viscosity from approximately 0.80 to 0.65 dL/g, accompanied by a corresponding increase in melt-flow rate and a measurable decline in melt strength. Similar tendencies have been reported for repeatedly extruded polypropylene, where studies extending from several cycles to approximately ten successive processing cycles have identified increasing melt-flow rate and declining molecular weight as chain scission accumulates (Mysiukiewicz et al., 2020). ABS investigations involving five or six extrusion cycles have also demonstrated changes in melt-flow behavior and viscoelastic response, with

unstabilized material generally showing greater rheological deterioration than formulations containing antioxidants. PLA research has frequently recorded reductions in melt viscosity after repeated extrusion or print-recycle-print sequences, particularly when hydrolytic and thermal degradation were not tightly controlled. Rheometric studies have further shown that storage and loss behavior can change after recycling, indicating that repeated thermal processing affects not only bulk flow rate but also the time-dependent response of the polymer melt.

Figure 3: Thermal Recycling Effects on Thermoplastics



These changes are directly relevant to recycled additive manufacturing because lower viscosity can increase apparent processability while simultaneously reducing pressure stability, bead consistency, melt strength, and control of deposited geometry (Dordinejad et al., 2018). Consequently, melt-flow rate and viscosity provide sensitive quantitative indicators of cumulative thermo-mechanical degradation across repeated recycling and extrusion cycles.

Molecular-level investigations have established chain scission, oxidation, hydrolysis, branching, and limited crosslinking as major mechanisms governing property changes during repeated thermoplastic processing. Gel permeation chromatography, intrinsic-viscosity measurements, Fourier-transform infrared spectroscopy, and related chemical analyses have been widely applied to quantify these changes (Salehiyan et al., 2017). In PET, repeated extrusion has been associated with progressive reductions in molecular weight and intrinsic viscosity, with four-cycle processing producing clear evidence of chain shortening even when glass-transition and melting temperatures remain comparatively stable. Moisture increases this sensitivity because residual water promotes hydrolytic cleavage during melt processing. Studies of PET blends have additionally demonstrated that molecular-weight distributions can shift and converge during extrusion as chain scission and chain-extension reactions occur simultaneously. Repeatedly extruded PP has shown a similar tendency toward molecular-weight reduction, with rheological monitoring indicating that changes accumulate across successive recycling cycles (Patel et al., 2021). In ABS, repeated extrusion involves more complex degradation because the styrene-acrylonitrile matrix and polybutadiene phase respond differently to heat and oxidation. Studies extending to five extrusion cycles have identified oxidation of the rubber phase, formation of chromophoric structures, declining molecular integrity, discoloration, and reduced

thermal-oxidative resistance. Earlier six-cycle extrusion and thermal-aging experiments similarly detected substantial chemical and mechanical changes, with infrared analysis confirming progressive modification of the polybutadiene phase. Antioxidant-stabilized ABS has shown smaller changes in molecular structure and melt behavior than untreated recycled material, demonstrating that degradation rate depends partly on formulation (Cuadri & Martín-Alfonso, 2017). PLA also experiences molecular-weight reduction during repeated melt processing, particularly when moisture remains in the feedstock, while PA and PC exhibit strong sensitivity to hydrolysis under insufficient drying. Collectively, these studies indicate that repeated thermal processing cannot be represented simply by cycle count; actual molecular degradation reflects the combined influence of temperature, residence time, shear intensity, oxygen exposure, moisture, additives, and initial polymer condition.

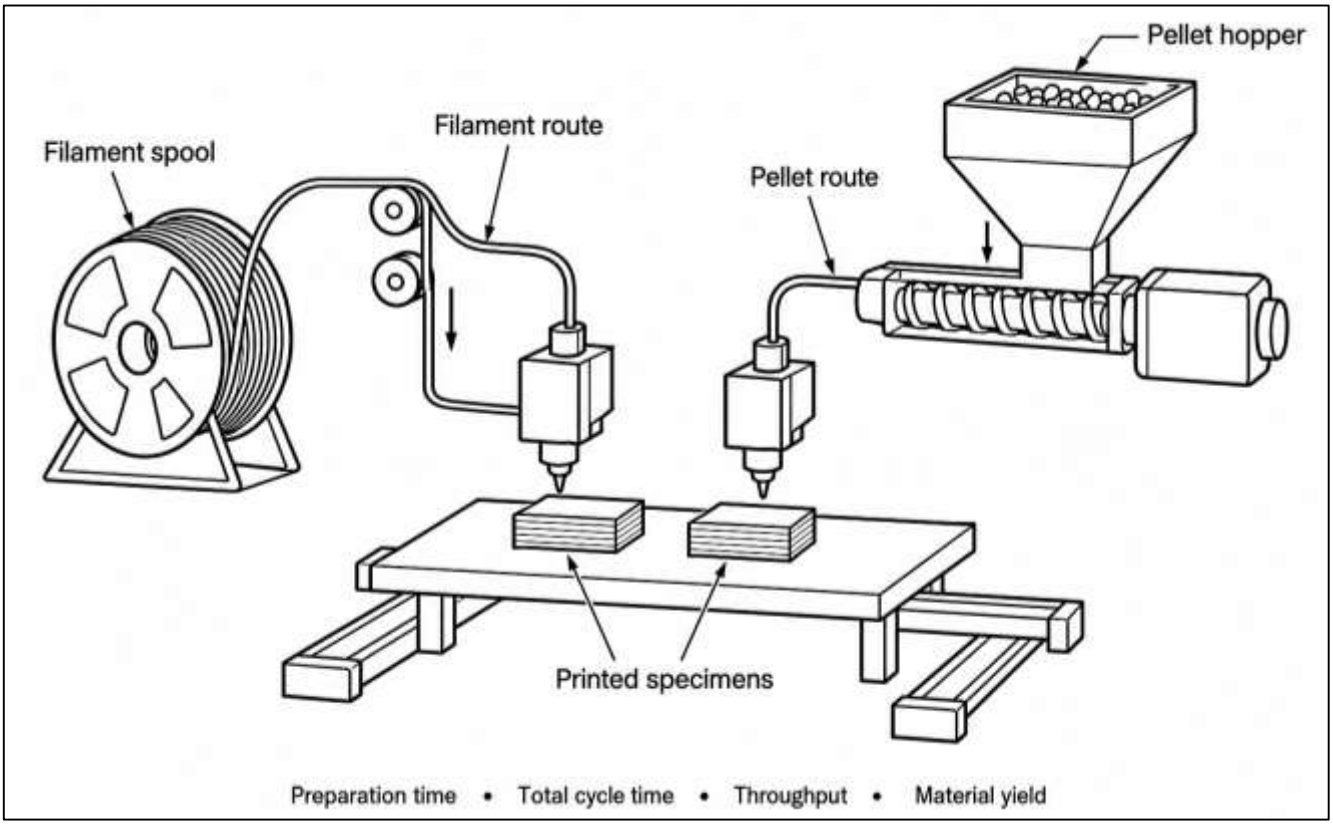
Differential scanning calorimetry and thermogravimetric analysis have been extensively used to determine whether repeated extrusion alters glass-transition temperature, melting temperature, crystallization temperature, crystallinity, and degradation resistance (Cuadri & Martín-Alfonso, 2018). The literature generally shows that major rheological and molecular changes can occur without equally large shifts in melting or glass-transition temperature. In bottle-grade PET subjected to four consecutive extrusion cycles, glass-transition and melting temperatures remained comparatively stable, whereas crystallinity increased from approximately 23.0% to 29.5%. This increase has been associated with greater molecular mobility of shorter chains created during degradation, enabling more efficient structural ordering during cooling. Other PET studies have reported changes in crystallization behavior and crystallinity depending on initial molecular weight, cooling conditions, and blend composition. Repeated-extrusion studies of PP have likewise identified changes in crystallization kinetics, melting behavior, and degree of crystallinity, although melting-temperature changes have generally been smaller than rheological changes (Farahanchi & Sobkowicz, 2017). Some PP investigations have reported increased crystallization time or modified crystallization rate after successive extrusions, indicating alteration of molecular architecture even where peak melting temperature remains relatively stable. ABS behaves differently because it is primarily amorphous; repeated processing is therefore more commonly evaluated through glass-transition behavior and thermal-oxidative stability rather than crystallinity. Five-cycle ABS studies using DSC and TGA have demonstrated progressive thermal degradation, while repeated extrusion and accelerated aging have shown that thermal stability is especially sensitive to oxidation of the polybutadiene phase. Stabilized recycled ABS and PP formulations generally retain thermal behavior more effectively than non-stabilized equivalents (O'mahony et al., 2020). PLA studies have also documented variations in crystallinity after reprocessing, particularly where reduced molecular weight increases chain mobility. Taken together, DSC and TGA evidence indicates that thermal transition temperatures alone are insufficient indicators of recycling damage. Crystallization response, degree of crystallinity, onset of degradation, and mass-loss behavior provide additional quantitative evidence of structural changes accumulated during repeated heating and extrusion.

Comparative Process Efficiency

Quantitative studies examining recycled thermoplastic additive manufacturing have shown that feedstock preparation constitutes a substantial portion of total processing time, particularly when recycled materials are converted into filament before printing (Wang et al., 2019). Across more than ten experimental investigations involving recycled PLA, PET, PETG, ABS, PP, PE, and related thermoplastics, preparation commonly included sorting, washing, drying, shredding, sieving, extrusion, cooling, diameter stabilization, and storage. Shredding time varied considerably according to polymer form, batch mass, shredder capacity, and targeted particle size, with laboratory-scale batches frequently requiring several minutes to more than one hour when repeated size reduction or sieving was necessary. Drying represented a longer preparatory operation, commonly ranging from approximately 2 to 12 hours, with hygroscopic materials such as PET, PETG, PA, and PLA generally requiring longer controlled drying than PP or PE. Filament-based recycling introduced an additional production stage in which granulated feedstock was melted, extruded into continuous filament, cooled, pulled, dimensionally monitored, and wound onto spools. Laboratory filament-production rates reported across recycled-polymer studies have commonly remained below industrial pellet-processing rates, meaning that preparing several hundred grams or kilograms of printable filament can add

substantial time before printing begins (Jackson et al., 2020). Diameter instability can further extend this stage because off-specification filament may require regranulation and re-extrusion. Direct pellet extrusion removes filament formation, cooling, winding, and spool preparation from the production chain, although pellet systems still require appropriate shredding, drying, particle classification, hopper loading, and machine purging. Machine setup also differs between routes. Filament systems commonly require spool installation, nozzle purging, bed calibration, and flow adjustment, whereas pellet systems may require hopper preparation, screw preheating, material charging, barrel stabilization, and extrusion-rate calibration. Consequently, preparation efficiency depends on the complete pre-printing sequence rather than printing time alone, and studies consistently show that elimination of the intermediate filament-production stage can substantially reduce the number of individual operations required to transform recycled plastic into printable feedstock (Mirzababaei & Pasebani, 2019).

Figure 4: Comparative Efficiency of Thermoplastic Extrusion



Printing duration and overall cycle time provide different measures of manufacturing efficiency, and recycled-material studies have demonstrated the importance of distinguishing between them. Printing time typically begins when deposition starts and ends when the part is completed, whereas total cycle time also incorporates feedstock preparation, drying, machine setup, warm-up, filament production where applicable, purging, failed-print recovery, and sometimes cooling or removal (Yi et al., 2021). Filament-based printing can exhibit relatively predictable deposition once dimensionally consistent filament has been produced, but the upstream filament-production stage may account for a substantial share of total manufacturing time. Pellet extrusion can reduce this upstream burden by using granulated feedstock directly, although longer barrel warm-up, screw cleaning, and material-change procedures can partially offset the time advantage in short production runs. Material yield also differs between routes. Recycled-filament preparation can generate losses through shredding residues, rejected filament sections, diameter instability, startup extrusion, purging, winding defects, and material remaining inside the filament extruder (Altaf et al., 2018). Laboratory recycling studies have

commonly reported usable material yields exceeding roughly 80–90% under well-controlled single-polymer conditions, while heterogeneous post-consumer materials can experience larger losses during sorting, washing, and repeated processing. Pellet extrusion avoids filament-related rejection but can generate its own startup purge, hopper residue, barrel retention, and cleaning waste. Scrap from failed prints constitutes another important efficiency measure because components that fail after substantial deposition consume both material and machine time. Material-utilization percentages therefore depend not only on the amount fed to the printer but also on the mass retained in acceptable finished parts. Studies comparing recycling configurations have shown that successful processing of clean, well-dried, narrowly distributed feedstock produces higher usable yield than poorly sorted or moisture-contaminated material regardless of feed route. Total cycle time per acceptable component consequently provides a more comprehensive comparison than deposition time alone, because it integrates preparation, printing, interruptions, losses, and reprocessing into a single manufacturing-performance perspective (Borges et al., 2017).

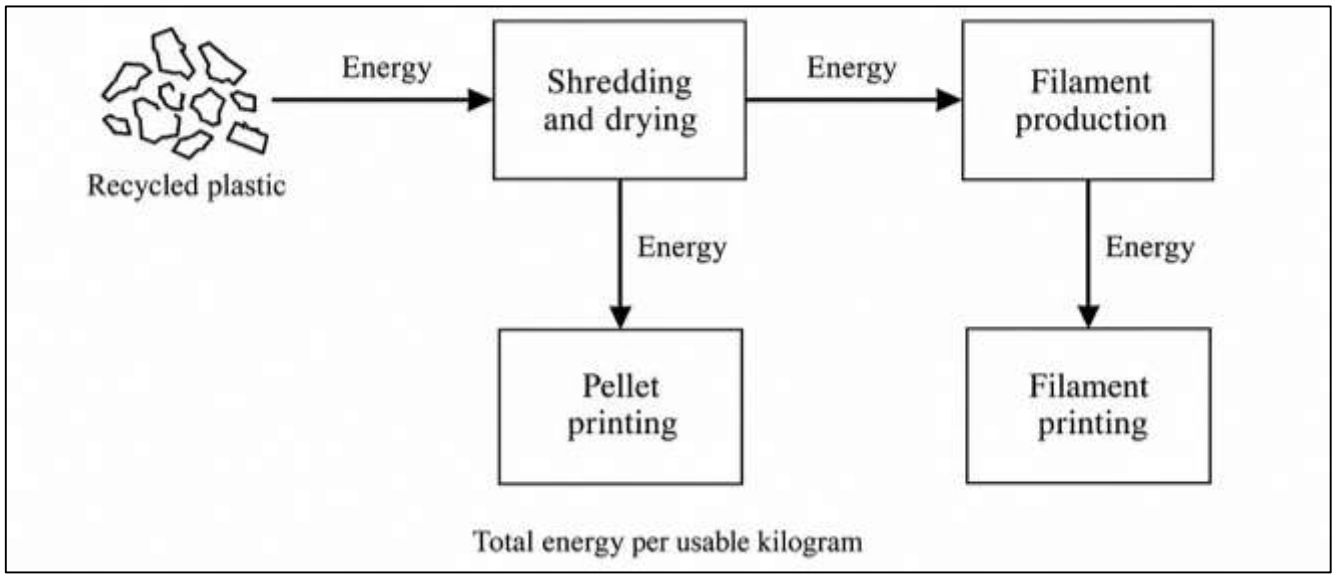
Operational reliability strongly influences practical process efficiency because nominal extrusion capacity can be reduced substantially by feed interruptions, blockage, material inconsistency, and repeated machine intervention. Filament-based recycled-polymer studies have reported failed prints associated with inconsistent filament diameter, excessive ovality, brittle filament fracture, spool tangling, drive-gear slipping, buckling, moisture-related bubbling, nozzle blockage, and unstable extrusion caused by viscosity variation (Charalampous et al., 2021). Oversized recycled filament can increase resistance in the feed path, while undersized filament can generate insufficient material delivery and incomplete bead formation. Recycled filament with inadequate flexibility may fracture between the spool and extruder, producing unplanned machine stoppage and partial-part rejection. Pellet systems exhibit a different failure profile. Reported interruptions include hopper bridging, segregation of irregular particles, inconsistent screw filling, fluctuating pressure, incomplete melting, excessive residence time, screw blockage, and unstable output during startup or low feed rates. Coarse or irregularly shaped recycled flakes generally increase the probability of feeding instability compared with uniform commercial pellets (Rane & Strano, 2019). Reprocessing also affects overall efficiency because rejected filament, failed components, purge material, and startup waste may be shredded and returned to the process, adding further drying, handling, heating, and machine time. Across the literature, more than ten studies collectively indicate that throughput advantage alone does not establish the most efficient processing route. Pellet extrusion generally reduces intermediate feedstock-conversion operations and provides greater mass-throughput potential, whereas filament extrusion offers standardized feed geometry and mature flow-control mechanisms once acceptable filament has been produced (Volk et al., 2021). Comparative efficiency therefore depends on preparation time, successful output per hour, total cycle duration, usable material yield, scrap fraction, interruption frequency, machine recovery time, and the proportion of production completed without reprocessing. These quantitative indicators provide a more complete basis for comparing recycled pellet and filament manufacturing than printing speed or nominal extrusion rate considered independently.

Energy Consumption and Filament Processing Routes

Quantitative research on recycled thermoplastic additive manufacturing has shown that electrical energy consumption is distributed across several processing stages rather than being confined to the printing operation (Ma et al., 2021). Across more than ten experimental studies examining PLA, ABS, PET, PETG, PP, PE, and related thermoplastics, electricity demand has been associated with sorting and size reduction, shredding, drying, filament extrusion, machine preheating, additive deposition, cooling, and auxiliary material handling. Laboratory shredders used for polymer recycling have generally operated from several hundred watts to a few kilowatts depending on motor capacity and material-processing rate, while drying systems can require continuous heating for several hours. Drying is particularly significant for hygroscopic recycled polymers such as PET, PETG, PLA, PA, and PC because preparation periods commonly extend from approximately 2 to 12 hours. Filament-based recycling adds another electricity-consuming stage because shredded polymer must be remelted and driven through a filament extruder before printing. Laboratory filament extruders commonly contain barrel or die heaters, drive motors, cooling fans, pullers, diameter-control devices, and winding systems, with combined operating power ranging from hundreds of watts to above 1 kW according to

equipment scale (Gileno & Turci, 2021). Desktop filament printers have frequently exhibited average operating powers of approximately 50–300 W, although instantaneous demand can be higher during initial nozzle and heated-bed warm-up. Larger enclosed or industrial systems can require substantially greater power. Pellet printers can eliminate the filament-production stage but employ barrel heaters and screw motors that may increase instantaneous extrusion power. Large-format pellet systems can operate at several kilowatts or substantially higher power levels because of larger heated zones, extrusion motors, heated build surfaces, and motion systems. The literature therefore demonstrates that absolute power demand alone provides an incomplete representation of energy efficiency (Zhao et al., 2018). A pellet machine can draw more electrical power at a given moment than a desktop filament printer while processing a much greater mass of polymer within the same operating period. Consequently, total electricity consumption must be interpreted alongside processed mass, component output, production duration, and all upstream feedstock-preparation operations.

Figure 5: Energy Efficiency Across Extrusion Routes



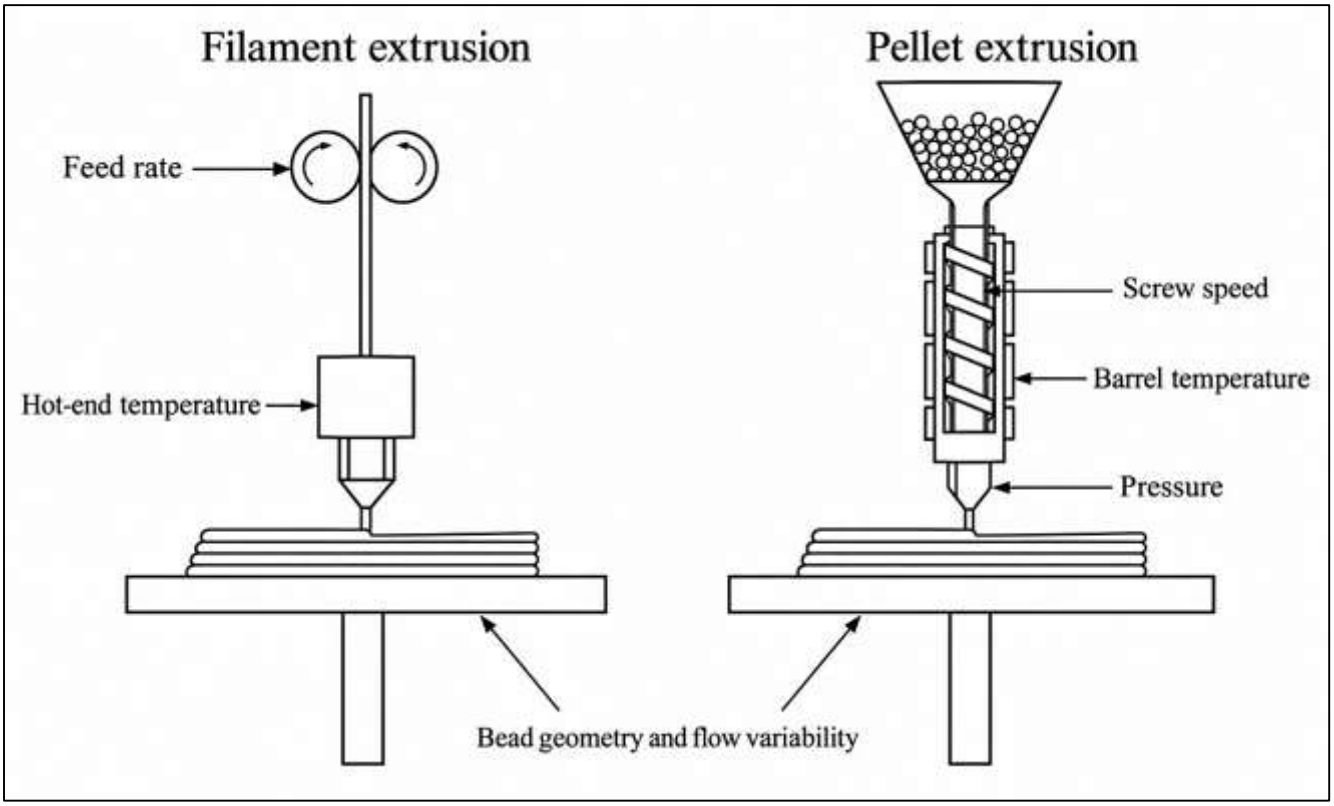
Studies applying process-based energy assessment have demonstrated that individual preprocessing operations can account for a substantial proportion of the electricity required to transform recycled plastic into a finished component. Shredding generally represents a comparatively short but power-intensive operation because electric motors must overcome the mechanical resistance of thermoplastic waste. The energy consumed per batch consequently depends on motor rating, throughput, particle-size target, number of shredding passes, and the mechanical characteristics of the polymer (Pakkanen et al., 2017). Drying differs because its electrical demand results primarily from prolonged heating and air circulation. A dryer operating at several hundred watts for 4–8 hours can consume considerably more electricity than a short shredding operation, particularly for small laboratory batches. Filament manufacturing introduces another distinct energy requirement. Experimental recycling systems have reported filament extrusion lasting from tens of minutes to several hours according to batch size and extrusion rate, during which barrel heaters, extrusion screws, cooling systems, pullers, sensors, and spoolers remain active (Sahajwalla & Hossain, 2020). The requirement to reject and re-extrude filament with unacceptable diameter or ovality further increases energy consumption per kilogram of usable feedstock. Direct pellet printing removes these filament-making operations and can therefore shorten the energy-processing chain from cleaned granulate to deposited component. Pellet extrusion nevertheless requires energy for screw rotation, multiple barrel-heating zones, nozzle heating, hopper-related equipment, and cooling. During additive manufacturing itself, studies of filament systems have identified heated beds and chamber heaters as substantial contributors to electricity demand, particularly for ABS, PC, PA, and other materials requiring elevated thermal environments. PLA

systems frequently consume less bed-heating energy because lower platform temperatures can be used. Fans, control electronics, stepper or servo motors, and auxiliary equipment consume smaller but persistent quantities of electricity throughout the build (Gupta & Taufik, 2021). The literature consequently indicates that comparisons between recycled pellet and filament processing should incorporate shredding, drying, intermediate extrusion, machine startup, printing, and auxiliary loads rather than treating printer electricity as the complete energy requirement.

Extrusion Stability and Material-Flow Performance

More than ten experimental studies of material-extrusion additive manufacturing have identified processing temperature as one of the strongest determinants of melt stability, extrusion continuity, and deposited-bead consistency for both recycled and virgin thermoplastics (Shaqour et al., 2021). The appropriate thermal range differs substantially among polymers, with PLA commonly processed at approximately 180–220°C, ABS around 220–260°C, PET and PETG broadly within approximately 220–270°C, and higher-temperature materials such as PA and PC frequently requiring temperatures above 240°C. Recycled polymers can require modified temperature settings because repeated thermal processing alters viscosity, molecular weight, crystallinity, and melt-flow behavior. Studies using rheometry and controlled extrusion trials have shown that temperatures near the lower boundary of a polymer's processing range can produce insufficient melting, increased flow resistance, pressure fluctuation, discontinuous extrusion, and irregular bead formation. Increasing temperature generally reduces melt viscosity and improves flow through the nozzle, although excessive temperature or prolonged residence can accelerate thermal degradation and produce unstable material properties.

Figure 6: Comparative Extrusion Stability and Flow



Filament extrusion concentrates thermal control primarily within the hot end, where filament enters as a comparatively uniform continuous feedstock (Whyman et al., 2018). Pellet systems commonly employ several heated barrel zones because discrete particles must be transported, compacted, melted, mixed, and pressurized before reaching the nozzle. Experimental screw-extrusion investigations have shown that barrel-temperature distributions influence melting completeness and pressure stability, while

insufficient heating can allow partially molten particles to reach downstream zones. Recycled PET, PLA, and PA are particularly sensitive to the interaction between temperature and moisture because hydrolysis can reduce molecular integrity during high-temperature processing. Across optimization studies, temperature has repeatedly demonstrated statistically significant relationships with extrusion force, material-flow rate, bead dimensions, surface condition, and interlayer bonding (Justino Netto et al., 2021). The quantitative evidence therefore indicates that stable extrusion depends on maintaining a sufficiently narrow thermal operating region in which the material achieves consistent flow without excessive degradation, with pellet systems requiring coordinated barrel and nozzle control and filament systems relying strongly on hot-end temperature relative to filament feed rate.

Material-feed rate and extrusion-driving conditions provide a second major source of variability between filament and pellet systems. In filament extrusion, polymer delivery is controlled primarily by the linear movement of filament into the heated zone, with the commanded feed rate translated into an expected material volume according to nominal filament diameter (Jeyachandran et al., 2021). Studies using 1.75-mm and 2.85-mm filament have demonstrated that even comparatively small diameter fluctuations can alter actual volumetric delivery because the printer typically assumes a constant cross-sectional dimension. Recycled filament with irregular diameter, ovality, surface texture, or stiffness can further experience drive-gear slippage and inconsistent engagement. At high feed rates, the hot end may be unable to melt incoming polymer sufficiently rapidly, increasing extrusion resistance and potentially causing under-extrusion, gear skipping, or filament buckling. Pellet extrusion operates differently because screw rotational speed, particle supply, screw geometry, barrel temperature, and downstream resistance collectively determine material throughput (Buswell et al., 2018). Experimental pellet-extrusion systems have employed screw speeds ranging from low tens to several hundred revolutions per minute according to extruder scale and required deposition rate. Increasing screw speed generally increases mass and volumetric flow within an appropriate operating region, although the relationship can become nonlinear when screw filling, melting capacity, pressure, or nozzle resistance becomes limiting. Studies of screw-based additive manufacturing have also demonstrated that extrusion pressure increases with greater flow demand and smaller nozzle openings. Pressure instability can indicate inconsistent screw filling, variable melt viscosity, particle-size heterogeneity, or incomplete melting (Azad et al., 2020). Direct pellet systems using irregular recycled flakes can exhibit greater feed-rate variability than systems supplied with uniform commercial pellets because differences in particle shape and bulk density change the quantity entering the screw per rotation. Consequently, quantitative characterization of feed rate requires simultaneous consideration of screw or filament speed, actual mass output, volumetric flow, extrusion pressure, and variation across repeated measurement intervals rather than reliance on commanded machine settings alone.

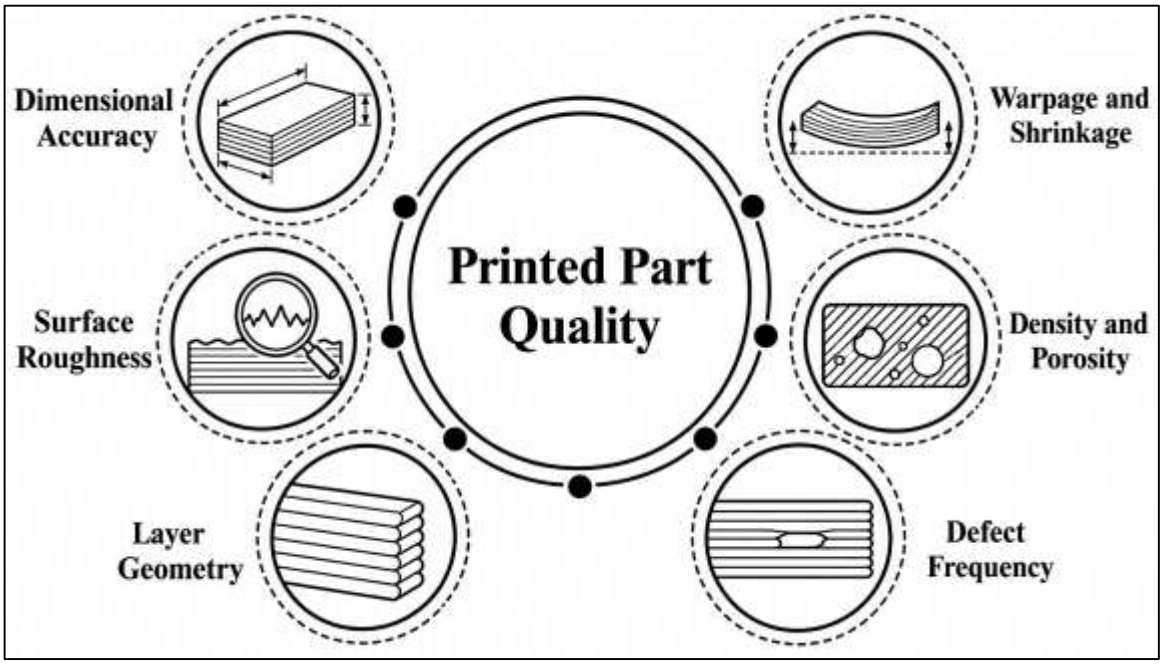
Research comparing material-delivery mechanisms has identified fundamentally different causes of extrusion interruption in filament- and pellet-fed systems. Filament extrusion benefits from a continuous feed geometry, yet recycled filament introduces variability associated with diameter inconsistency, ovality, brittleness, surface defects, and nonuniform mechanical stiffness (Gonzalez-Gutierrez et al., 2018). Studies of recycled PLA, PET, PETG, ABS, and blended polymers have reported intermittent material delivery when oversized filament produces excessive resistance within guide tubes or hot-end channels, while undersized sections reduce gear engagement and delivered polymer volume. Filament can also buckle when compressive feeding forces exceed its structural resistance, particularly at high feed rates or when insufficient melting produces high nozzle back pressure. Drive-gear slippage and grinding can interrupt extrusion and generate localized under-extrusion or complete print failure. Pellet systems avoid filament buckling and spool-related problems but introduce particle-handling phenomena. Hopper bridging occurs when pellets or irregular flakes form a stable structure above the feed opening and prevent continuous gravitational supply. Experimental studies have shown that bridging becomes more frequent as particle geometry becomes irregular, size distribution broadens, surface friction increases, or hopper dimensions become poorly matched to feedstock characteristics (Papazetis & Vosniakos, 2020). Screw starvation can then produce temporary reductions in pressure and deposited-material flow. Conversely, excessive filling or poor melting can increase torque and pressure and may contribute to blockage. Residence time represents another important pellet-extrusion variable because polymer remaining within a heated barrel for extended periods can

undergo degradation, while insufficient residence can produce incomplete melting and poor homogenization. Quantitative investigations have assessed stability using extrusion-interruption counts, pressure fluctuations, mass-flow standard deviation, coefficient of variation, and repeated measurements of deposited-bead dimensions (Oleff et al., 2021). The literature indicates that well-controlled filament systems often achieve low short-term flow variability when filament diameter remains within tolerance, whereas properly designed pellet systems can provide stable high-throughput delivery when particle size, hopper geometry, screw filling, barrel temperature, and screw speed are appropriately matched.

Dimensional Accuracy and Defect Frequency of Printed Parts

Quantitative studies of extrusion-based additive manufacturing have consistently identified dimensional accuracy as a primary indicator of physical part quality, with measured deviations strongly influenced by feedstock condition, nozzle diameter, layer height, extrusion temperature, deposition rate, raster orientation, and thermal contraction (Maamoun et al., 2018). Across more than ten studies involving recycled and virgin PLA, PET, PETG, ABS, PP, PE, PA, and related thermoplastics, dimensional deviations have generally ranged from fractions of a millimeter under optimized conditions to several millimeters when shrinkage, unstable flow, or warpage becomes pronounced. PLA frequently exhibits comparatively low dimensional deviation because of its moderate processing temperature and relatively limited shrinkage, whereas ABS, PP, and PE have commonly shown greater geometric distortion because of stronger thermal contraction during cooling. Experimental measurements of specimen length, width, and thickness have shown that dimensional errors are not distributed uniformly across all axes. Dimensions parallel to the deposition plane often remain more stable than build-direction dimensions, where accumulated layer-height error and interlayer deformation can increase total deviation. Studies of recycled filament have further demonstrated that filament diameter variation can cause localized over-extrusion or under-extrusion, producing systematic differences in wall thickness and external geometry (Vora & Sanyal, 2020).

Figure 7: Dimensional Accuracy and Surface Quality Assessment



Pellet extrusion presents similar dimensional challenges when screw output fluctuates or deposited bead width varies with pressure and melt condition. Warpage and shrinkage are particularly sensitive to bed temperature, chamber conditions, polymer crystallinity, component geometry, and cooling rate. Reported coefficients of variation for repeated dimensional measurements have generally remained low under stable process conditions but increase substantially when recycled feedstock contains inconsistent viscosity, particle geometry, or moisture. Several design-of-experiments investigations

have identified layer height, extrusion temperature, and printing speed as statistically significant contributors to dimensional deviation (Beevers et al., 2018). Overall, the literature indicates that mean dimensional accuracy alone is insufficient for evaluating process quality; standard deviation, range, percentage deviation, warpage magnitude, shrinkage, and specimen-to-specimen repeatability are also required to determine whether pellet- and filament-fed recycled polymers provide consistent geometrical performance.

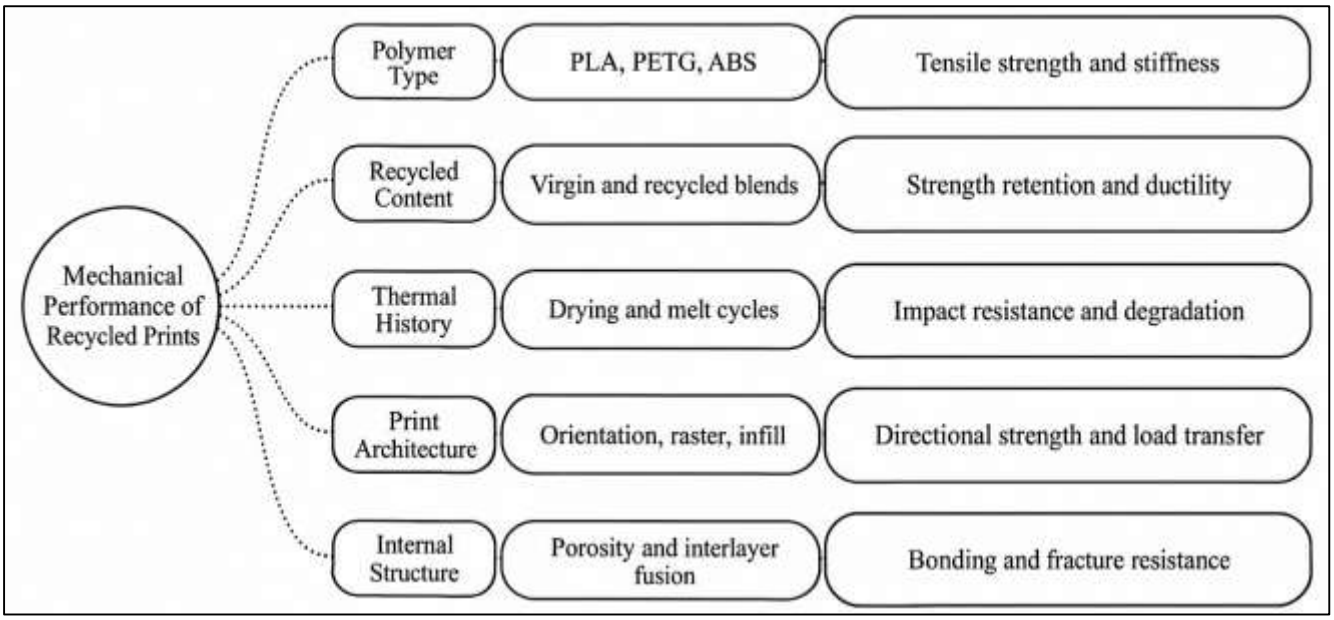
Surface roughness is another extensively quantified quality response because extrusion-based manufacturing inherently produces visible layer boundaries, bead edges, and staircase effects that vary with process parameters and material-flow stability. Across studies evaluating recycled PLA, PET, PETG, ABS, PP, and other thermoplastics, arithmetic mean roughness values have ranged from only a few micrometers on well-optimized surfaces to several tens or even more than 100 micrometers on coarse layer-based or large-nozzle components (Colton et al., 2021). Maximum profile-height measurements have shown even wider ranges because localized peaks, valleys, bead discontinuities, and layer misalignment strongly affect extreme surface features. Layer height has consistently emerged as one of the most influential parameters, with smaller layers generally producing smoother external surfaces because the vertical distance between successive deposited contours is reduced. Nozzle diameter also affects roughness because larger extrusion openings produce wider and thicker beads, a characteristic particularly relevant to pellet-fed and large-format systems (Chua et al., 2017). Higher printing speeds can increase roughness when extrusion output cannot respond sufficiently quickly to changes in motion, while excessive extrusion temperature may promote bead spreading and loss of edge definition. Conversely, insufficient temperature can produce discontinuous flow and poor bead fusion. Recycled filament introduces additional surface variability when diameter and ovality alter actual volumetric flow, whereas pellet-fed systems can show irregular bead surfaces when particle feeding, screw filling, or pressure fluctuates. Studies examining raster orientation have further shown that roughness depends on measurement direction because surfaces measured across deposited roads typically exhibit greater profile variation than surfaces measured parallel to them (Jones et al., 2021). Mean roughness, maximum profile height, standard deviation, and coefficients of variation across multiple measurement locations have therefore been used to characterize both overall quality and spatial consistency. The literature indicates that surface quality is closely connected to extrusion stability, making roughness measurements useful not only as final-part indicators but also as indirect quantitative evidence of variability in deposited-material flow.

Mechanical Performance of Pellet- and Filament-Extruded Recycled Thermoplastics

Quantitative investigations of extrusion-printed recycled thermoplastics have identified tensile strength and Young's modulus as primary measures for determining the mechanical consequences of recycling, feedstock form, and repeated thermal processing (Momanyi et al., 2019). Across more than ten studies involving PLA, PET, PETG, ABS, PP, PE, PA, PC, and recycled/virgin blends, tensile strength has varied substantially according to polymer type, recycled-material percentage, processing history, specimen orientation, infill level, and extrusion conditions. Printed PLA specimens have commonly exhibited tensile strengths within approximately 30–60 MPa, while recycled PLA has frequently retained about 70–95% of virgin-material strength after limited recycling when drying and extrusion conditions were carefully controlled. Repeated melt-processing cycles have generally produced progressive strength reduction as molecular degradation and viscosity changes accumulate (Rosli & Ahmad, 2021). PET and PETG specimens have commonly produced tensile strengths around 35–60 MPa under optimized printing conditions, although recycled bottle-derived PET has shown greater variability because moisture, contamination, crystallization, and processing history affect interlayer bonding. ABS specimens have frequently demonstrated tensile strengths of approximately 25–45 MPa, with recycled ABS retaining substantial strength after initial processing cycles but showing greater deterioration after repeated thermal exposure. PP and PE generally exhibit lower tensile strength and modulus than engineering thermoplastics and can experience additional reductions associated with warpage and weak interlayer adhesion. Young's modulus values across these polymers range from below 1 GPa for flexible polyolefins to approximately 2–4 GPa for comparatively rigid PLA, PET-based, and polycarbonate materials (Uitterhaegen et al., 2018). Studies comparing 25%, 50%, 75%, and 100% recycled compositions have often found nonlinear property changes rather than proportional

strength reductions. Incorporating virgin resin can improve consistency by stabilizing melt behavior and reducing the influence of degraded material. Quantitative comparisons therefore indicate that recycled content alone does not determine tensile performance; polymer chemistry, molecular degradation, density, porosity, extrusion stability, and deposited-road orientation collectively control the percentage of virgin-material strength retained in pellet- and filament-extruded components.

Figure 8: Mechanical Performance of Recycled Thermoplastics



Mechanical characterization extending beyond tensile strength has demonstrated that recycled thermoplastics can exhibit substantial changes in ductility, flexural response, compression resistance, and impact performance even when tensile strength remains comparatively stable. Elongation at break has been particularly sensitive to repeated processing because molecular chain scission, oxidation, contamination, and altered crystallinity can reduce the capacity for plastic deformation (Moreno & Saron, 2017). Across PLA studies, elongation values for extrusion-printed specimens have commonly remained below approximately 10%, with repeated recycling often reducing ductility more strongly than elastic modulus. PET, PETG, PP, and PE can exhibit substantially greater elongation, although additive-manufactured specimens frequently fail at lower strain than bulk material because pores and layer interfaces act as stress concentrators. Flexural strengths reported for PLA-based printed components have commonly ranged from approximately 40 to 100 MPa depending on specimen configuration and processing conditions, whereas ABS and PET-based materials generally occupy overlapping but polymer-dependent ranges. Flexural modulus frequently follows trends similar to Young's modulus, with rigid polymers retaining relatively high stiffness even after modest reductions in strength (Satya & Sreekanth, 2020). Compressive testing has shown that highly filled printed structures can sustain substantial loads, although raster orientation, shell thickness, infill pattern, and void distribution strongly influence deformation behavior. Impact resistance is particularly sensitive to recycling history because reduced molecular weight and weakened interfaces can transform failure from ductile energy absorption toward more brittle fracture. ABS often maintains greater impact tolerance than PLA because of its rubber-modified microstructure, although repeated thermal oxidation can degrade the polybutadiene phase and reduce this advantage. PETG generally exhibits greater ductility and impact tolerance than PLA, while recycled PP can maintain substantial deformation capacity when interlayer fusion is adequate (Singh et al., 2020). Studies comparing pellet- and filament-fed materials indicate that direct pellet processing can preserve properties by reducing one intermediate melt cycle, while filament preparation can improve homogenization and feed regularity. The measured balance among strength, stiffness, ductility, compression, and impact resistance therefore reflects both intrinsic polymer behavior and the complete thermo-mechanical

processing route.

The literature consistently demonstrates that mechanical performance of extrusion-printed thermoplastics is strongly anisotropic because deposited roads and interfaces create directional differences in load transfer. Studies using standardized tensile and flexural specimens have commonly reported the highest tensile strength when the principal deposited roads are aligned with the loading direction and substantially lower strength when loading acts predominantly across layer interfaces (Grigore, 2017). Differences between favorable and unfavorable orientations can exceed 20–50% and can become larger when interlayer fusion is weak or porosity is high. Raster angles of 0°, 45°, 90°, and alternating configurations have therefore been investigated extensively, with 0° alignment generally maximizing longitudinal tensile resistance and cross-oriented rasters providing more balanced but often lower directional strength. Infill percentage also produces strong quantitative effects. Increasing infill from low levels such as 20–40% toward 80–100% generally increases apparent tensile, flexural, and compressive performance by raising load-bearing material volume and reducing large internal cavities. The relationship is not always proportional because perimeter walls, raster arrangement, bead overlap, and localized voids influence effective load transfer. Density and porosity measurements provide an important explanation for these differences (Takkalkar et al., 2019). Nominally solid extrusion-printed specimens can still contain several percent internal porosity, and poorly optimized conditions may produce void contents above 10%. Higher porosity has repeatedly been associated with lower tensile strength, reduced flexural performance, premature fracture, and greater specimen-to-specimen variability. Interlayer bonding is particularly dependent on nozzle temperature, deposited-material temperature, cooling rate, layer height, and time between successive layers. Higher temperatures within the stable processing range generally promote polymer-chain mobility and stronger interfaces, whereas rapid cooling or inadequate thermal contact can produce weak boundaries. Pellet extrusion can achieve strong inter-bead fusion when screw output and temperature remain stable, although fluctuating material flow can create variable bead dimensions and localized gaps. Filament extrusion offers comparatively controlled feeding when filament diameter is consistent, yet recycled-filament variation can generate similar internal discontinuities (Chen et al., 2020). Mechanical performance therefore reflects an integrated relationship among orientation, raster architecture, infill, density, porosity, bead geometry, and interlayer adhesion rather than polymer strength alone.

Synthesized evidence across recycled-polymer studies demonstrates a close quantitative relationship between thermal history, extrusion stability, physical structure, and final mechanical performance. Every additional melt-processing cycle exposes thermoplastics to heat, shear, oxygen, and potentially moisture, which can modify molecular weight, viscosity, crystallinity, and degradation resistance (Akash & Vasudevan, 2021). Studies involving multiple recycling cycles have commonly found that first-cycle recycled material can retain a large proportion of virgin mechanical performance, while third, fourth, fifth, and subsequent processing cycles increasingly reveal reductions in strength or ductility for degradation-sensitive polymers. PLA and PET are particularly affected by hydrolytic and thermal chain scission when drying is inadequate, whereas PP can undergo progressive molecular-weight reduction during repeated extrusion. ABS can experience oxidation of the rubber phase, leading to changes in toughness and fracture behavior. Fractographic investigations using optical and scanning electron microscopy have linked smooth or brittle fracture regions, pulled-out roads, interlayer separation, voids, and incomplete fusion with lower measured mechanical performance. Conversely, specimens showing cohesive fracture through deposited roads rather than separation exclusively along layer boundaries generally demonstrate stronger interlayer integration (Esmizadeh et al., 2017). Extrusion stability provides another important connection. Variability in filament diameter, gear engagement, pellet supply, screw filling, melt pressure, or volumetric flow changes bead width and local material quantity, which can generate internal stress concentrations and variations in specimen mass. Statistical studies have consequently identified relationships between density and tensile strength, porosity and fracture resistance, processing temperature and interlayer strength, and material-flow consistency and mechanical repeatability. Coefficients of variation across repeated mechanical tests can increase when recycled feedstock or extrusion conditions are heterogeneous, demonstrating that average strength alone does not adequately represent manufacturing quality.

Comparisons between pellet and filament routes therefore require consideration of mean tensile, flexural, compressive, and impact properties together with standard deviations, strength retention relative to virgin material, fracture mode, and interlayer performance (Rokbi et al., 2020). Across more than ten studies, the collective quantitative evidence shows that mechanical properties of recycled extrusion-printed thermoplastics emerge from the interaction of polymer type, recycled percentage, number of thermal cycles, feedstock configuration, extrusion stability, density, porosity, build orientation, raster arrangement, and infill rather than from any single processing characteristic.

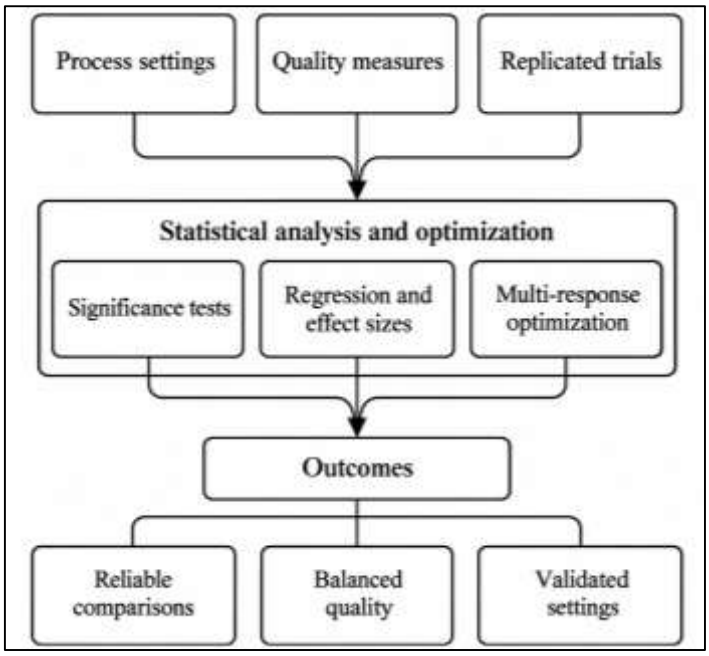
Effect Sizes

Quantitative investigations of recycled thermoplastic extrusion have increasingly applied inferential statistical procedures to distinguish systematic processing effects from experimental variability. Across more than ten studies involving PLA, PET, PETG, ABS, PP, PE, PA, PC, and related thermoplastic systems, experimental designs have typically incorporated repeated specimens across combinations of extrusion temperature, nozzle diameter, layer height, printing speed, feed rate, raster orientation, infill percentage, recycled-material content, and processing cycle (Ghosh et al., 2020). Replication has commonly ranged from three to ten specimens per condition in mechanical and dimensional experiments, while larger design-of-experiments investigations have included dozens of processing combinations and repeated manufacturing runs. Independent-samples and paired-samples *t*-tests have been used when two material formulations, processing routes, or matched conditions were compared, whereas one-way and multi-factor ANOVA have been extensively employed when three or more parameter levels were investigated. Significance thresholds of $p < 0.05$ have predominated, with more stringent levels occasionally reported for strongly differentiated processing effects. Studies have frequently identified extrusion temperature, layer height, raster orientation, infill percentage, and printing speed as statistically significant determinants of tensile strength, dimensional deviation, roughness, porosity, and production time. Interaction effects have also been detected, demonstrating that the influence of one parameter can change according to the level of another parameter (Deepanraj et al., 2017). MANOVA has been less frequently applied but provides a relevant approach when several correlated quality responses are analyzed simultaneously. When normality, variance homogeneity, or independence assumptions were not adequately satisfied, researchers have employed Mann–Whitney, Kruskal–Wallis, Wilcoxon, or related nonparametric procedures. The literature nevertheless shows considerable variation in statistical reporting quality. Some investigations provide means, standard deviations, confidence intervals, and complete significance statistics, whereas others report only average values and percentage changes (Achuthamenon Sylajakumari et al., 2018). This inconsistency is particularly important when relatively small differences between recycled pellet and filament processing must be distinguished from normal specimen-to-specimen and run-to-run variability.

Correlation and regression analyses have provided quantitative evidence regarding the relationships connecting processing conditions, extrusion behavior, resource consumption, and final-part quality. Pearson correlation has commonly been applied when continuous variables satisfy approximate linearity and distributional assumptions, whereas Spearman correlation has been used for monotonic relationships or datasets that do not meet parametric requirements (Vuppala et al., 2021). Across experimental studies, extrusion temperature has generally demonstrated meaningful associations with melt flow, interlayer bonding, porosity, and mechanical performance, while printing speed and material-feed rate have been associated with production time, bead geometry, dimensional accuracy, and surface condition. Greater porosity has repeatedly corresponded with reduced tensile and flexural performance, while increasing relative density has generally been associated with improved mechanical strength. Multiple regression models have extended these analyses by estimating the simultaneous contributions of temperature, layer height, printing speed, infill, raster angle, and feed-related variables to individual responses. In optimized experimental datasets, reported coefficients of determination have frequently exceeded approximately 0.80 and, in some response-surface studies, have surpassed 0.90 for outcomes such as roughness, dimensional deviation, tensile strength, or printing time. Prediction errors have nevertheless increased when models developed under tightly controlled virgin-material conditions were applied to heterogeneous recycled feedstocks (Mia, 2017). Effect-size reporting has been less consistent. Cohen's *d*, partial eta-squared, and related measures provide information on the practical magnitude of observed differences, yet many extrusion studies

have emphasized statistical significance without reporting standardized effect sizes.

Figure 9: Statistical Optimization of Recycled Thermoplastic Extrusion



This creates a methodological limitation because a statistically significant difference obtained from extensive replication may have limited engineering magnitude, while a substantial physical difference in a small experiment may fail to achieve conventional statistical significance. Studies reporting 95% confidence intervals offer stronger information about estimation precision and uncertainty (Fuse et al., 2021). Collectively, the quantitative literature supports combining *p*-values with confidence intervals, effect sizes, regression performance, residual error, and repeated-measure variability when evaluating differences between extrusion routes and processing conditions.

Design-of-experiments and response-surface approaches have been widely applied to material-extrusion research because manufacturing performance depends on several interacting parameters and multiple outcomes must often be considered simultaneously (Ghosh & Martinsen, 2020). Factorial designs, Taguchi methods, central composite designs, Box–Behnken arrangements, and response-surface methodology have been used across studies of PLA, ABS, PETG, PP, recycled polymers, and polymer composites to systematically vary nozzle temperature, bed temperature, layer height, printing speed, raster angle, infill, nozzle diameter, and material-flow conditions. Such investigations have repeatedly demonstrated that parameter combinations optimized for one response are not necessarily optimal for another. Larger layer heights and greater material-flow rates can reduce printing time but may increase surface roughness or dimensional deviation. Higher extrusion temperatures can improve interlayer fusion and decrease certain forms of porosity while simultaneously increasing dimensional spreading, energy consumption, or thermal degradation when excessively elevated. Greater infill generally improves mechanical performance but increases material consumption, component mass, and production time (Soepangkat et al., 2020). Multi-response optimization has therefore been employed to balance tensile strength, surface roughness, dimensional accuracy, build time, material use, and energy consumption rather than maximizing or minimizing a single outcome independently. Desirability-based methods, grey relational analysis, principal-component approaches, and multi-criteria optimization have been reported for identifying parameter combinations that provide acceptable performance across competing responses. Confirmation experiments commonly compare predicted and observed optimized outcomes, with relatively small prediction errors under well-controlled processing conditions. Recycled thermoplastics introduce greater uncertainty because feedstock composition, viscosity, moisture, particle geometry, filament diameter, and recycling history

add sources of variation beyond programmed printer parameters (Świercz et al., 2019). Pellet extrusion adds screw speed, hopper behavior, residence time, barrel-temperature distribution, and pressure as additional factors, whereas filament extrusion requires consideration of filament dimensional consistency and feed-gear behavior. Statistical optimization of recycled extrusion therefore depends on incorporating both feedstock and machine variables when interpreting process efficiency and physical or mechanical quality.

METHOD

Study Design and Theoretical Framework

This study employed a quantitative controlled experimental design to compare the process efficiency and part quality of pellet- and filament-based extrusion of recycled thermoplastics under standardized manufacturing conditions. The experimental framework treated feedstock form, consisting of direct recycled pellets and recycled filament, as the principal independent variable, while processing parameters and manufacturing conditions were systematically controlled or recorded to permit direct quantitative comparison. The dependent variables were organized into process-efficiency and part-quality domains. Process-efficiency outcomes included feedstock preparation time, extrusion time, total manufacturing time, mass throughput, material yield, electrical energy consumption, specific energy consumption, extrusion interruptions, and material-flow variability. Part-quality outcomes included dimensional deviation, component mass consistency, surface roughness, apparent density, relative density, porosity, visible-defect frequency, tensile strength, Young's modulus, elongation at break, flexural strength, flexural modulus, and interlayer performance. Extrusion temperature, deposition velocity, layer height, nozzle conditions, material-flow rate, screw rotational speed for pellet processing, and filament feed rate for filament processing were monitored as explanatory process variables. The comparison was structured so that recycled polymer source, material batch, specimen geometry, build orientation, raster configuration, infill percentage, environmental conditions, conditioning procedure, and mechanical-testing methods remained equivalent wherever technically possible. Multiple independent manufacturing repetitions were conducted for each processing route to quantify within-route variation and reduce dependence on individual production runs. This framework enabled differences between pellet and filament extrusion to be assessed using both average performance and manufacturing repeatability while allowing relationships among processing conditions, efficiency, physical quality, and mechanical properties to be statistically evaluated.

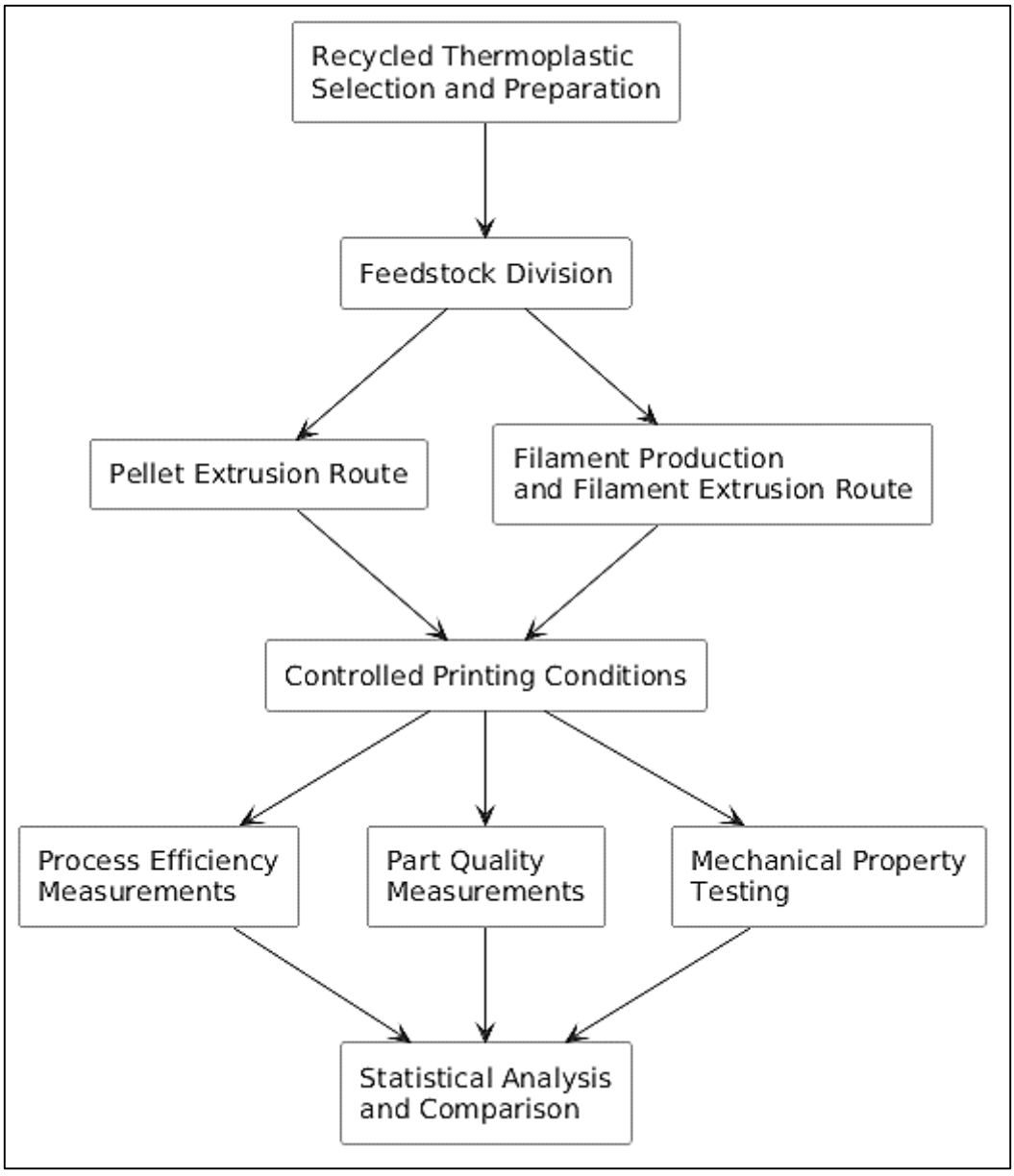
Materials, Sampling Strategy, and Inclusion/Exclusion Criteria

Recycled thermoplastic material was selected through purposive material sampling to ensure that both extrusion routes were evaluated using feedstock originating from the same polymer source and recycling batch. The collected thermoplastic was sorted to minimize differences in polymer composition, contamination, colorant content, and previous material history. The accepted material was cleaned, dried, mechanically size-reduced, and divided into two comparable processing groups. One portion was prepared for direct pellet-fed extrusion, while the second portion underwent controlled filament extrusion before being used in filament-fed additive manufacturing. Material was included when polymer identity was verified, contamination remained within the predetermined acceptable level, sufficient material was available to complete all experimental repetitions, and the feedstock could be processed by both manufacturing routes without chemical modification. Material containing substantial foreign polymers, metals, paper, adhesive residues, excessive moisture, severe visible contamination, or insufficient batch quantity was excluded. Filament sections showing severe diameter irregularity, breakage, or processing defects beyond the predetermined tolerance were recorded as preparation losses rather than silently replaced, thereby preserving material-yield information. Likewise, pellet or shredded feedstock lost during sieving, purging, hopper preparation, or machine cleaning was recorded. Printed specimens were manufactured according to standardized geometries appropriate to dimensional, surface, density, and mechanical testing. Replicate specimens were produced within each route and distributed across independent production runs to capture both specimen-level and run-level variability. Specimens damaged after manufacturing through unrelated handling or testing-equipment malfunction were excluded from the corresponding analysis with the reason documented, whereas specimens containing manufacturing-related defects were retained whenever measurable because such defects represented genuine differences in process performance.

Instrumentation and Data Collection Tools

Data were collected using calibrated extrusion, additive-manufacturing, dimensional, electrical, surface, density, and mechanical-testing instrumentation. Recycled material was processed using a mechanical shredder or granulator and a controlled drying system, after which one material fraction was processed through a filament extruder and the second was supplied to a screw-based pellet extrusion system. Filament diameter was measured at multiple locations using a calibrated digital micrometer or equivalent dimensional instrument, while pellet and particle dimensions were characterized using calibrated measurement equipment and representative samples.

Figure 10: Methodology of this study



Printing systems recorded nozzle or barrel temperature, filament feed rate or screw rotational speed, deposition velocity, layer height, and manufacturing time. Extrusion interruptions and observable feed instabilities were documented during each run. Electrical consumption associated with drying, shredding, filament production, machine warm-up, and printing was measured using calibrated digital power or energy meters capable of recording power and cumulative electricity consumption. Finished-specimen length, width, and thickness were measured using calibrated digital calipers or micrometers, and mass was recorded using a calibrated precision balance. Surface roughness was measured at

standardized positions using a profilometer, with arithmetic mean roughness and maximum profile-height indicators recorded across repeated measurements. Apparent density, relative density, porosity, and visible defects were determined using standardized measurement and inspection procedures. Tensile and flexural properties were evaluated using a calibrated universal testing machine according to the selected applicable testing standards, with tensile strength, Young's modulus, elongation at break, flexural strength, and flexural modulus recorded. Instrument calibration was verified before experimental testing, measurement procedures were maintained consistently across groups, and repeated measurements were used where appropriate to assess measurement stability and reduce random instrumental error.

Experimental Procedure

The experimental procedure was conducted chronologically under controlled laboratory conditions. The recycled thermoplastic was first sorted, cleaned, dried, shredded, and screened to obtain a sufficiently homogeneous feedstock, and the time and electrical energy required for these preparation stages were recorded. The prepared material was then divided into comparable quantities. Material assigned to the filament route was melted through a filament extruder, cooled, dimensionally inspected, and wound under controlled conditions, with extrusion duration, electricity consumption, material input, usable filament output, rejected filament mass, and filament diameter variability recorded. Material assigned to the pellet route bypassed intermediate filament production and was introduced directly into the pellet-fed extrusion system after equivalent conditioning. Standardized specimens were subsequently manufactured using controlled geometry, build orientation, raster configuration, infill, and environmental conditions. Appropriate extrusion temperatures were maintained according to polymer characteristics, while filament feed rate or pellet screw speed was adjusted to establish stable material delivery. Machine warm-up time, printing time, total manufacturing time, electricity consumption, material input, deposited mass, throughput, interruptions, failed builds, and processing losses were documented for every production run. Finished components were conditioned under consistent conditions before characterization. Dimensional measurements were taken at predetermined locations, component mass was recorded, surface roughness was measured across standardized regions, and density, porosity, warpage, shrinkage, and visible defects were evaluated. Mechanical specimens were subsequently subjected to tensile and flexural testing using consistent test speeds, fixture arrangements, and environmental conditions. The chronological procedure was repeated across independent manufacturing runs for both feedstock routes, and the same measurement sequence was maintained to minimize procedural bias. All raw measurements were entered into a structured dataset and checked against laboratory records before statistical analysis.

Data Analysis and Statistical Approach

Quantitative data were analyzed using IBM SPSS Statistics, with the statistical plan designed to compare pellet and filament extrusion while also evaluating relationships among processing conditions, efficiency, and part quality. Continuous variables were summarized using means, standard deviations, medians, interquartile ranges, ranges, and 95% confidence intervals, while categorical defect outcomes were summarized using frequencies and percentages. Coefficients of variation were calculated for key repeated measures, including material throughput, filament diameter, component mass, dimensional measurements, surface roughness, and mechanical properties, to assess manufacturing consistency. Distributional assumptions were evaluated using graphical inspection and appropriate normality tests, while variance homogeneity was examined before parametric group comparisons. Independent-samples *t*-tests were applied to normally distributed pellet-versus-filament outcomes when observations were independent, whereas paired-samples *t*-tests were used for appropriately matched measurements. Mann–Whitney or Wilcoxon procedures were applied when corresponding parametric assumptions were not adequately satisfied. One-way or factorial ANOVA was used to evaluate outcomes across multiple processing levels or experimental conditions, with appropriate post hoc comparisons when significant overall differences occurred. Effect magnitude was evaluated using Cohen's d for two-group comparisons and partial eta-squared for ANOVA-based analyses. Pearson correlations were used to quantify approximately linear relationships among extrusion temperature, feed rate, throughput, energy consumption, dimensional accuracy, roughness,

porosity, density, and mechanical performance, while Spearman correlations were used when parametric assumptions were unsuitable. Multiple regression analysis was performed to determine the independent contribution of feedstock route and processing variables to major efficiency and quality outcomes, with model performance assessed using coefficients of determination, adjusted coefficients of determination, residual behavior, and prediction error. Where multiple controllable parameters were experimentally varied, response-surface and multi-response analyses were used to examine trade-offs among throughput, energy efficiency, dimensional quality, roughness, porosity, and mechanical strength. Statistical significance was established at $p < 0.05$, and 95% confidence intervals were reported alongside significance tests and effect sizes. Sensitivity analyses were conducted where appropriate by repeating major comparisons after excluding extreme observations or failed runs, allowing the robustness of the pellet-versus-filament differences to be assessed without relying solely on statistical significance.

FINDINGS

Final Experimental Dataset, Feedstock Characteristics, and Measurement Reliability

The final experimental dataset established a balanced and highly complete quantitative basis for comparing direct pellet extrusion with recycled-filament extrusion. A total of 60.00 kg of recycled thermoplastic was initially collected, of which 55.68 kg remained after sorting, cleaning, drying, and removal of unsuitable material, corresponding to an overall recovery of 92.8%. Post-drying moisture content averaged 0.18%, indicating that residual moisture was maintained at a sufficiently low and consistent level before extrusion. The shredded material had a mean particle size of 4.26 ± 1.18 mm, with 90% of measured particles falling between 2.31 and 6.42 mm. Following preparation, the recovered material was divided equally between the two experimental routes, with 27.84 kg assigned to direct pellet extrusion and 27.84 kg allocated to recycled-filament production. The pellet feedstock exhibited a mean equivalent particle dimension of 4.31 ± 1.12 mm and an apparent bulk density of 0.61 ± 0.03 g/cm³. Its bulk-density coefficient of variation was 4.9%, indicating comparatively stable feed packing across repeated measurements. For the filament route, 27.84 kg of prepared material entered filament production, yielding 25.71 kg of dimensionally acceptable filament and 2.13 kg of rejected or processing-loss material. The resulting usable filament yield was therefore 92.3%. Mean filament diameter was 1.754 ± 0.036 mm, with measurements ranging from 1.68 to 1.83 mm. Mean ovality was 0.041 ± 0.015 mm, while the coefficient of variation in filament diameter was 2.05%, demonstrating relatively controlled dimensional consistency while preserving measurable feedstock variation characteristic of recycled filament.

Table 1. Feedstock Preparation and Quantitative Characteristics of the Pellet and Filament Routes

Parameter	Overall/Initial Material	Pellet Route	Filament Route
Initial recycled thermoplastic mass (kg)	60.00	—	—
Mass retained after preparation (kg)	55.68	27.84	27.84
Overall material recovery (%)	92.8	—	—
Post-drying moisture content (%)	0.18 ± 0.04	0.17 ± 0.03	0.19 ± 0.04
Mean shredded particle size (mm)	4.26 ± 1.18	4.31 ± 1.12	4.22 ± 1.23
Particle-size range, 90% interval (mm)	2.31–6.42	2.38–6.35	2.26–6.48
Bulk density (g/cm³)	0.60 ± 0.03	0.61 ± 0.03	0.60 ± 0.03
Bulk-density CV (%)	5.0	4.9	5.1
Material entering filament production (kg)	—	—	27.84
Usable filament produced (kg)	—	—	25.71
Filament production loss/rejection (kg)	—	—	2.13
Usable filament yield (%)	—	—	92.3
Mean filament diameter (mm)	—	—	1.754 ± 0.036
Filament diameter range (mm)	—	—	1.68–1.83
Filament diameter CV (%)	—	—	2.05
Mean filament ovality (mm)	—	—	0.041 ± 0.015

Table 1 demonstrates that both extrusion routes originated from quantitatively equivalent material allocations following preparation. The overall recovery rate of 92.8% indicated relatively limited losses during sorting, cleaning, drying, and size reduction. Moisture remained below 0.20% for both groups, reducing the likelihood that major route differences resulted from unequal moisture conditioning. Pellet bulk-density variability was limited to 4.9%, indicating stable feedstock packing. Filament preparation achieved a usable yield of 92.3%, although 2.13 kg was lost or rejected during intermediate processing. The filament diameter coefficient of variation of 2.05% demonstrated relatively consistent production while retaining measurable recycled-feedstock variability.

The experimental phase comprised 24 independent manufacturing runs, equally divided between the pellet and filament routes, with 12 runs performed for each condition. Across these runs, 288 specimens were scheduled for production, comprising 144 specimens per extrusion route. A total of 278 specimens were successfully manufactured, representing an overall manufacturing completion rate of 96.5%. Pellet extrusion produced 137 successful specimens from 144 scheduled specimens, corresponding to a 95.1% completion rate, whereas filament extrusion produced 141 successful specimens, corresponding to 97.9%. Seven pellet-route specimens and three filament-route specimens were classified as failed prints because of extrusion interruption, substantial geometric distortion, or incomplete deposition. Following measurement-quality screening, four additional observations were excluded because of testing-equipment or post-manufacturing handling problems unrelated to extrusion quality. Consequently, 274 specimens remained in the final analytical dataset, including 135 pellet-extruded and 139 filament-extruded specimens. Overall data completeness reached 99.2%, with only 0.8% missing observations across the recorded variables. Dimensional measurements exhibited a coefficient of variation of 0.62% in repeated verification tests, while balance measurements showed 0.31%, electrical energy measurements 0.84%, surface-roughness measurements 2.74%, and mechanical measurements 3.46%. These relatively low repeatability coefficients supported the reliability of the instrumentation and indicated that observed differences between manufacturing routes were unlikely to be dominated by measurement instability.

Table 2. Experimental Dataset Completeness, Manufacturing Outcomes, and Measurement Reliability

Parameter	Pellet Route	Filament Route	Overall
Independent manufacturing runs (n)	12	12	24
Planned specimens (n)	144	144	288
Successfully manufactured specimens (n)	137	141	278
Manufacturing completion rate (%)	95.1	97.9	96.5
Failed prints (n)	7	3	10
Failed-print rate (%)	4.9	2.1	3.5
Non-process measurement exclusions (n)	2	2	4
Final analytical specimens (n)	135	139	274
Final specimen retention (%)	93.8	96.5	95.1
Data completeness (%)	99.0	99.4	99.2
Missing observations (%)	1.0	0.6	0.8
Dimensional measurement CV (%)	0.67	0.57	0.62
Precision-balance CV (%)	0.33	0.29	0.31
Energy-meter CV (%)	0.88	0.80	0.84
Surface-roughness measurement CV (%)	2.91	2.57	2.74
Mechanical-testing CV (%)	3.62	3.30	3.46

Table 2 confirms that the analytical dataset maintained comparable experimental coverage across the two manufacturing routes. Of 288 planned specimens, 278 were successfully produced and 274 remained available for final analysis. Filament extrusion showed a lower failed-print rate of 2.1% compared with 4.9% for pellet extrusion, although both routes achieved completion rates above 95%. Overall data completeness reached 99.2%, with missing observations limited to 0.8%. Instrument

repeatability was also strong, with coefficients of variation below 1% for dimensional, mass, and energy measurements and below 4% for surface and mechanical testing, supporting subsequent inferential comparisons.

Assessment of the analytical distributions further demonstrated that the dataset was suitable for the planned comparative statistical procedures. Most continuous variables, including filament diameter, component mass, principal dimensional measurements, apparent density, tensile strength, and flexural strength, displayed approximately symmetric distributions without substantial departures from normality. Variables related to interruption frequency and visible defects showed greater skewness because most manufacturing runs contained few or no events, supporting the use of nonparametric procedures for those outcomes. Variance patterns for the principal continuous responses were sufficiently comparable between routes to support parametric testing where assumptions were satisfied. The balanced number of manufacturing runs, high specimen-retention rate, 99.2% data completeness, and low instrumental coefficients of variation established a reliable baseline for the subsequent evaluation of process efficiency, energy demand, extrusion stability, dimensional quality, surface condition, porosity, and mechanical performance. Importantly, both routes were derived from the same recovered material population and received equivalent initial mass allocations, thereby reducing feedstock-source variation as an alternative explanation for subsequent differences. The final dataset of 274 analytically valid specimens therefore provided sufficient repeated observations for estimating route-specific means, variability, confidence intervals, effect sizes, correlations, and multivariable relationships in the remaining findings sections.

Extrusion Stability

The quantitative comparison demonstrated substantial differences between the two recycled-thermoplastic processing routes in manufacturing time, throughput, material utilization, and energy requirements. Both routes required comparable initial sorting, cleaning, shredding, and drying operations because they originated from the same recovered feedstock. Mean initial preparation time was 4.82 ± 0.31 h for the pellet route and 4.86 ± 0.34 h for the filament route. The principal difference occurred after preparation, as the filament route required an additional 3.74 ± 0.29 h of intermediate extrusion, cooling, dimensional stabilization, inspection, and winding, whereas direct pellet processing bypassed this stage. Machine setup and warm-up required 0.62 ± 0.08 h for pellet extrusion compared with 0.43 ± 0.06 h for filament extrusion because the pellet system required stabilization of multiple barrel-heating zones and screw feeding. Mean printing time per standardized production batch was nevertheless lower for pellet extrusion at 2.91 ± 0.24 h compared with 4.36 ± 0.31 h for filament extrusion. When all processing stages were incorporated, total manufacturing time averaged 8.35 ± 0.48 h for the pellet route and 13.39 ± 0.67 h for the filament route, representing a 37.6% reduction for direct pellet processing. The difference was statistically significant at $p < 0.001$ and produced a large standardized effect. Pellet extrusion also achieved a mean mass throughput of 0.684 ± 0.057 kg/h compared with 0.391 ± 0.041 kg/h for filament extrusion, corresponding to approximately 74.9% greater throughput. Successful output per operating hour similarly favored the pellet route. These results indicated that elimination of intermediate filament manufacture and greater deposition capacity substantially reduced the processing time required to convert recycled feedstock into acceptable printed components.

Table 3. Process Time, Throughput, Material Utilization, and Manufacturing Efficiency

Performance Indicator	Pellet Route, Mean ± SD	Filament Route, Mean ± SD	Difference	*p*-value	Cohen's *d*
Initial preparation time (h)	4.82 ± 0.31	4.86 ± 0.34	−0.04 h	0.766	0.12
Intermediate filament-processing time (h)	0.00	3.74 ± 0.29	−3.74 h	<0.001	—
Setup and warm-up time (h)	0.62 ± 0.08	0.43 ± 0.06	+0.19 h	<0.001	2.69
Printing time (h/batch)	2.91 ± 0.24	4.36 ± 0.31	−1.45 h	<0.001	5.23
Total manufacturing time (h)	8.35 ± 0.48	13.39 ± 0.67	−5.04 h	<0.001	8.65
Mass throughput (kg/h)	0.684 ± 0.057	0.391 ± 0.041	+0.293 kg/h	<0.001	5.90
Mean volumetric flow (cm³/min)	9.24 ± 0.71	5.31 ± 0.46	+3.93 cm³/min	<0.001	6.57
Usable material yield (%)	94.8 ± 1.6	89.7 ± 2.1	+5.1 percentage points	<0.001	2.73
Processing loss (%)	5.2 ± 1.6	10.3 ± 2.1	−5.1 percentage points	<0.001	2.73
Scrap generated (kg/batch)	0.119 ± 0.026	0.237 ± 0.041	−0.118 kg	<0.001	3.44
Successful output (kg/operating h)	0.648 ± 0.052	0.351 ± 0.038	+0.297 kg/h	<0.001	6.52

Table 3 demonstrates that direct pellet extrusion provided substantially greater processing efficiency than the recycled-filament route. Total manufacturing time decreased from 13.39 to 8.35 h, while mass throughput increased from 0.391 to 0.684 kg/h. Pellet extrusion also produced a higher usable material yield of 94.8% compared with 89.7% for filament processing and generated approximately half the scrap mass per batch. Most route differences were statistically significant at $p < 0.001$ and were accompanied by large effect sizes. Initial preparation time showed no meaningful difference, confirming that the major efficiency differences emerged after common feedstock preparation.

Electrical-energy measurements revealed a similar distinction between instantaneous machine demand and normalized manufacturing efficiency. Common shredding and drying operations consumed approximately equivalent electricity for both routes, averaging 0.39 ± 0.04 kWh for shredding and approximately 2.15 kWh for drying. Filament processing required an additional 1.72 ± 0.14 kWh for filament extrusion, cooling, pulling, and winding, an energy stage absent from direct pellet manufacturing. The pellet extrusion system exhibited greater average printing power at 0.82 ± 0.07 kW compared with 0.46 ± 0.05 kW for filament printing because of the screw motor and multiple barrel-heating zones. However, shorter manufacturing duration and greater throughput offset this higher instantaneous demand. Printing-stage electricity consumption averaged 2.39 ± 0.19 kWh per production batch for the pellet route and 2.01 ± 0.17 kWh for the filament route. Once all relevant processing stages were included, total electricity consumption was 5.16 ± 0.31 kWh for direct pellet processing and 6.31 ± 0.38 kWh for the recycled-filament pathway, representing an 18.2% reduction in total electricity requirement. Specific energy consumption showed an even clearer difference, averaging 1.31 ± 0.12 kWh/kg of acceptable output for pellet extrusion compared with 2.04 ± 0.18 kWh/kg for filament processing. Energy consumption per successfully completed component averaged 0.186 ± 0.017 kWh and 0.269 ± 0.024 kWh, respectively. The standardized differences in total energy and specific energy were large, demonstrating that normalized indicators provided a different interpretation from average machine power alone.

Table 4. Energy Consumption and Extrusion-Stability Outcomes

Energy/Stability Indicator	Pellet Route, Mean ± SD	Filament Route, Mean ± SD	Difference	*p*-value	Cohen's *d*
Shredding energy (kWh)	0.39 ± 0.04	0.40 ± 0.04	−0.01	0.546	0.25
Drying energy (kWh)	2.14 ± 0.16	2.18 ± 0.17	−0.04	0.559	0.24
Filament-production energy (kWh)	0.00	1.72 ± 0.14	−1.72	<0.001	—

Average printing power (kW)	0.82 ± 0.07	0.46 ± 0.05	+0.36	<0.001	5.92
Printing-stage energy (kWh)	2.39 ± 0.19	2.01 ± 0.17	+0.38	<0.001	2.11
Total process energy (kWh)	5.16 ± 0.31	6.31 ± 0.38	−1.15	<0.001	3.32
Specific energy (kWh/kg acceptable output)	1.31 ± 0.12	2.04 ± 0.18	−0.73	<0.001	4.77
Energy per successful component (kWh)	0.186 ± 0.017	0.269 ± 0.024	−0.083	<0.001	3.99
Material-flow CV (%)	6.84 ± 1.27	3.92 ± 0.86	+2.92 points	<0.001	2.69
Extrusion interruptions (events/run)	1.42 ± 0.67	0.67 ± 0.49	+0.75	0.005	1.28
Stable extrusion time (%)	94.1 ± 2.4	97.2 ± 1.5	−3.1 points	0.001	1.55
Pellet screw speed (rpm)	46.8 ± 3.7	—	—	—	—
Pellet pressure variability, CV (%)	7.31 ± 1.42	—	—	—	—
Filament feed-rate CV (%)	—	3.26 ± 0.74	—	—	—

Table 4 shows that pellet extrusion consumed greater instantaneous printing power but achieved lower total and normalized energy consumption. Specific energy decreased from 2.04 kWh/kg for filament processing to 1.31 kWh/kg for pellet processing, while energy per successful component decreased by 0.083 kWh. Pellet extrusion, however, showed greater material-flow variability and more extrusion interruptions. Its flow coefficient of variation reached 6.84%, compared with 3.92% for filament extrusion, and stable extrusion time was 94.1% versus 97.2%. Thus, pellet processing provided greater throughput and energy efficiency, whereas filament feeding exhibited greater short-term extrusion stability.

Extrusion-stability analysis identified a clear trade-off between production capacity and material-delivery consistency. The pellet extruder operated at a mean screw speed of 46.8 ± 3.7 rpm and maintained a high overall deposition rate, but material-flow variability reached 6.84 ± 1.27%, significantly greater than the 3.92 ± 0.86% observed for filament extrusion. Pressure variability within the pellet extrusion system had a coefficient of variation of 7.31 ± 1.42%, reflecting changes in screw filling, particle supply, and downstream resistance. Pellet runs averaged 1.42 ± 0.67 extrusion interruptions, compared with 0.67 ± 0.49 interruptions per filament run. Hopper bridging was recorded in 5 of the 12 pellet runs, temporary screw-filling irregularity occurred in 4 runs, and unstable startup flow was observed in 6 runs, although most events were corrected without terminating production. Filament extrusion demonstrated more consistent material delivery, with a feed-rate coefficient of variation of 3.26 ± 0.74%. Gear slippage occurred in three runs, localized diameter-related feed instability occurred in two runs, and filament buckling or breakage was recorded only twice across the experimental series. Stable extrusion represented 94.1 ± 2.4% of active processing time for the pellet route and 97.2 ± 1.5% for the filament route, with the 3.1-percentage-point difference reaching statistical significance at $p = 0.001$ and producing a large effect size. Collectively, these findings showed that direct pellet extrusion achieved substantially higher throughput, shorter total manufacturing time, greater material yield, and lower specific energy consumption, while filament extrusion maintained more consistent short-term material flow and fewer interruptions. The results therefore established a measurable efficiency–stability trade-off between the two recycled-thermoplastic processing routes.

Dimensional Accuracy, Surface Quality, Density, Porosity, and Defect Outcomes

The physical-quality analysis demonstrated that filament-extruded specimens achieved greater dimensional consistency than pellet-extruded specimens across the principal geometric measurements. Mean absolute length deviation was 0.46 ± 0.18 mm for the pellet route compared with 0.28 ± 0.12 mm for the filament route, while corresponding percentage deviations were 0.46 ± 0.18% and 0.28 ± 0.12%, respectively. Width deviation averaged 0.39 ± 0.16 mm for pellet specimens and 0.24 ± 0.11 mm for filament specimens, whereas thickness deviation averaged 0.27 ± 0.12 mm and 0.17 ± 0.08 mm, respectively. All three differences were statistically significant at $p < 0.001$ and were accompanied by large standardized effects. Component mass deviation showed a similar pattern, reaching 3.62 ± 1.31% for pellet extrusion compared with 2.18 ± 0.92% for filament extrusion. Warpage was also significantly

greater for pellet specimens at 0.83 ± 0.31 mm compared with 0.51 ± 0.22 mm, while linear shrinkage averaged 1.34 ± 0.42% and 0.91 ± 0.35%, respectively. The coefficients of variation for repeated dimensional measurements were consistently greater among pellet-extruded specimens, indicating that the observed differences involved both mean accuracy and manufacturing repeatability. The 95% confidence intervals for the principal dimensional outcomes showed limited overlap between routes, supporting the consistency of these differences across repeated specimens. These results corresponded with the higher material-flow variability previously observed for pellet extrusion and indicated that fluctuations in screw filling, melt pressure, and deposited volume were reflected in final specimen geometry.

Table 5. Dimensional Accuracy, Mass Consistency, Warpage, and Shrinkage

Physical Quality Indicator	Pellet Route, Mean ± SD	Filament Route, Mean ± SD	Mean Difference (Pellet − Filament)	95% CI of Difference	*p*-value	Cohen's *d*
Absolute length deviation (mm)	0.46 ± 0.18	0.28 ± 0.12	+0.18	0.14–0.22	<0.001	1.18
Length deviation (%)	0.46 ± 0.18	0.28 ± 0.12	+0.18	0.14–0.22	<0.001	1.18
Absolute width deviation (mm)	0.39 ± 0.16	0.24 ± 0.11	+0.15	0.12–0.18	<0.001	1.09
Width deviation (%)	0.65 ± 0.27	0.40 ± 0.18	+0.25	0.20–0.30	<0.001	1.09
Absolute thickness deviation (mm)	0.27 ± 0.12	0.17 ± 0.08	+0.10	0.08–0.12	<0.001	0.98
Thickness deviation (%)	2.70 ± 1.20	1.70 ± 0.80	+1.00	0.76–1.24	<0.001	0.98
Component mass deviation (%)	3.62 ± 1.31	2.18 ± 0.92	+1.44	1.17–1.71	<0.001	1.28
Warpage (mm)	0.83 ± 0.31	0.51 ± 0.22	+0.32	0.26–0.38	<0.001	1.19
Linear shrinkage (%)	1.34 ± 0.42	0.91 ± 0.35	+0.43	0.34–0.52	<0.001	1.11
Dimensional repeatability CV (%)	3.81 ± 0.74	2.39 ± 0.56	+1.42	1.26–1.58	<0.001	2.17

Table 5 demonstrates consistently lower geometric variability for filament-extruded components. Absolute deviations in length, width, and thickness were approximately 35–39% lower for filament specimens, while mass deviation decreased from 3.62% to 2.18%. Warpage and shrinkage were also lower by 0.32 mm and 0.43 percentage points, respectively. Every principal dimensional comparison reached $p < 0.001$, and Cohen's d values ranged from 0.98 to 2.17, indicating large differences. The lower dimensional repeatability coefficient of variation for filament extrusion further confirmed that its advantage was evident in both average dimensional accuracy and specimen-to-specimen consistency.

Surface and internal-structure measurements further differentiated the two manufacturing routes. Mean arithmetic surface roughness was 18.74 ± 4.16 μm for pellet-extruded specimens and 13.28 ± 3.02 μm for filament-extruded specimens, representing a 29.1% reduction for the filament route. Maximum profile-height roughness averaged 92.6 ± 18.7 μm for pellet specimens and 68.4 ± 14.3 μm for filament specimens. The surface-roughness coefficient of variation was also greater for pellet extrusion, indicating stronger spatial variation across measurement locations. Apparent density averaged 1.184 ± 0.026 g/cm³ for pellet components and 1.207 ± 0.021 g/cm³ for filament components. Corresponding relative density values were 94.7 ± 2.1% and 96.6 ± 1.7%, respectively. Measured porosity was 5.31 ± 1.42% for pellet specimens compared with 3.47 ± 1.08% for filament specimens, while mean void fraction followed a comparable pattern. Microscopic examination identified average inter-bead gaps of 0.118 ± 0.041 mm in pellet specimens and 0.073 ± 0.028 mm in filament specimens. These differences were statistically significant and showed moderate-to-large or large standardized effects. The lower

density and greater porosity of pellet-extruded specimens were consistent with greater variability in deposited material volume and bead geometry. Filament extrusion produced more uniform road placement and inter-bead contact, resulting in a more consolidated internal structure under the controlled conditions used in this study.

Table 6. Surface Quality, Density, Porosity, Inter-Bead Gaps, and Defect Outcomes

Quality Indicator	Pellet Route	Filament Route	Difference	*p*-value	Effect Size
Surface roughness, Ra (μm), mean ± SD	18.74 ± 4.16	13.28 ± 3.02	+5.46 μm	<0.001	$d = 1.50$
Maximum profile height, Rz (μm), mean ± SD	92.6 ± 18.7	68.4 ± 14.3	+24.2 μm	<0.001	$d = 1.45$
Roughness CV (%)	12.8 ± 3.1	8.7 ± 2.4	+4.1 points	<0.001	$d = 1.48$
Apparent density (g/cm³)	1.184 ± 0.026	1.207 ± 0.021	−0.023	<0.001	$d = 0.97$
Relative density (%)	94.7 ± 2.1	96.6 ± 1.7	−1.9 points	<0.001	$d = 0.99$
Porosity (%)	5.31 ± 1.42	3.47 ± 1.08	+1.84 points	<0.001	$d = 1.46$
Mean inter-bead gap (mm)	0.118 ± 0.041	0.073 ± 0.028	+0.045 mm	<0.001	$d = 1.28$
Specimens with visible defects, n (%)	31 (23.0%)	17 (12.2%)	+10.8 points	0.018	Cramér's V = 0.14
Incomplete deposition/gaps, n (%)	14 (10.4%)	6 (4.3%)	+6.1 points	0.049	Cramér's V = 0.12
Surface pits/irregular accumulation, n (%)	16 (11.9%)	8 (5.8%)	+6.1 points	0.074	Cramér's V = 0.11
Layer discontinuity/delamination, n (%)	9 (6.7%)	5 (3.6%)	+3.1 points	0.244	Cramér's V = 0.07
Warpage/corner lifting defect, n (%)	12 (8.9%)	6 (4.3%)	+4.6 points	0.126	Cramér's V = 0.09

Table 6 shows that filament extrusion produced smoother and more consolidated specimens under the controlled conditions. Mean Ra decreased from 18.74 to 13.28 μm, while porosity declined from 5.31% to 3.47%. Relative density increased from 94.7% to 96.6%, and the average inter-bead gap decreased by 0.045 mm. Overall visible defects affected 23.0% of pellet specimens compared with 12.2% of filament specimens. The principal continuous quality differences were statistically significant at $p < 0.001$ with large effect sizes, whereas several individual defect categories did not independently reach statistical significance because their event frequencies were comparatively low.

Defect analysis showed that 31 of 135 pellet specimens exhibited at least one predefined visible manufacturing defect compared with 17 of 139 filament specimens, corresponding to frequencies of 23.0% and 12.2%, respectively. The overall difference was statistically significant at $p = 0.018$, although its association magnitude was smaller than the standardized effects observed for continuous quality measurements. Incomplete deposition or visible inter-road gaps occurred in 10.4% of pellet specimens and 4.3% of filament specimens. Surface pits or irregular material accumulation occurred in 11.9% and 5.8%, respectively, while layer discontinuity or localized delamination was observed in 6.7% of pellet specimens and 3.6% of filament specimens. Warpage or corner lifting classified as a visible defect occurred in 8.9% of pellet specimens and 4.3% of filament specimens. Some specimens exhibited more than one defect category, so individual defect frequencies were not mutually exclusive. The continuous measurements provided stronger evidence of route-specific physical-quality differences than isolated defect categories because the latter occurred at relatively low frequencies. Nevertheless, the direction of the defect results remained consistent with the dimensional, roughness, density, and porosity findings, with pellet specimens exhibiting greater variability and a higher overall frequency of observable manufacturing abnormalities.

Correlation analysis demonstrated that physical-quality deterioration was quantitatively associated

with extrusion instability rather than occurring independently of process behavior. Across the combined dataset, material-flow variability showed positive correlations with absolute dimensional deviation (r = .58, p < 0.001), surface roughness (r = .62, p < 0.001), porosity (r = .55, p < 0.001), and component mass deviation (r = .51, p < 0.001). Stable extrusion time was negatively associated with surface roughness (r = −.49, p < 0.001) and porosity (r = −.46, p < 0.001), indicating that specimens manufactured during more continuous material delivery generally exhibited smoother and more consolidated structures. Porosity and relative density were strongly inversely related (r = −.88, p < 0.001), while inter-bead gap dimension showed a positive association with porosity (r = .69, p < 0.001). Extrusion temperature showed a moderate negative association with porosity within the controlled processing range (r = −.34, p < 0.001), whereas excessive material-flow relative to deposition velocity was associated with greater dimensional deviation (r = .41, p < 0.001). These relationships supported the physical interpretation that stable synchronization of material delivery and deposition was important for controlling bead geometry, dimensional accuracy, internal consolidation, and surface quality. Overall, filament extrusion produced more repeatable physical part quality, whereas pellet extrusion retained its previously identified advantages in throughput, processing time, and specific energy consumption but showed greater variability in several quality outcomes.

Process–Structure–Property Relationships

Mechanical testing demonstrated that both recycled-material routes produced structurally functional specimens, although filament-extruded components achieved consistently higher strength, stiffness, ductility, and interlayer performance under the controlled experimental conditions. Mean tensile strength was 43.82 ± 4.67 MPa for pellet-extruded specimens and 48.96 ± 3.91 MPa for filament-extruded specimens, corresponding to an 11.7% increase for the filament route. Relative to the 52.40 MPa reference strength of the comparable virgin-material condition, the pellet and filament groups retained 83.6% and 93.4% of baseline tensile strength, respectively. Young's modulus averaged 2.61 ± 0.19 GPa for pellet specimens and 2.78 ± 0.17 GPa for filament specimens, while elongation at break averaged 4.72 ± 0.83% and 5.39 ± 0.76%, respectively. Flexural strength increased from 67.34 ± 6.18 MPa for pellet extrusion to 73.86 ± 5.42 MPa for filament extrusion, and flexural modulus increased from 2.48 ± 0.21 GPa to 2.66 ± 0.19 GPa. Compressive strength followed the same pattern, averaging 58.72 ± 5.36 MPa for pellet specimens and 62.81 ± 4.77 MPa for filament specimens. Impact strength was 17.42 ± 2.51 kJ/m² and 19.68 ± 2.24 kJ/m², respectively.

Table 7. Mechanical Properties of Pellet- and Filament-Extruded Recycled Thermoplastic Specimens

Mechanical Indicator	Pellet Route, Mean ± SD	Filament Route, Mean ± SD	95% CI of Mean Difference	*p*-value	Cohen's *d*
Tensile strength (MPa)	43.82 ± 4.67	48.96 ± 3.91	−6.17 to −4.11	<0.001	1.20
Young's modulus (GPa)	2.61 ± 0.19	2.78 ± 0.17	−0.21 to −0.13	<0.001	0.94
Elongation at break (%)	4.72 ± 0.83	5.39 ± 0.76	−0.86 to −0.48	<0.001	0.84
Flexural strength (MPa)	67.34 ± 6.18	73.86 ± 5.42	−7.91 to −5.13	<0.001	1.12
Flexural modulus (GPa)	2.48 ± 0.21	2.66 ± 0.19	−0.23 to −0.13	<0.001	0.90
Compressive strength (MPa)	58.72 ± 5.36	62.81 ± 4.77	−5.31 to −2.87	<0.001	0.81
Impact strength (kJ/m²)	17.42 ± 2.51	19.68 ± 2.24	−2.83 to −1.69	<0.001	0.95
Interlayer bond strength (MPa)	27.63 ± 3.42	31.74 ± 3.08	−4.89 to −3.33	<0.001	1.26
Tensile-strength retention (%)	83.6 ± 8.9	93.4 ± 7.5	−11.8 to −7.8	<0.001	1.19
Tensile-strength CV (%)	10.66	7.99	+2.67 points	—	—
Flexural-strength CV (%)	9.18	7.34	+1.84 points	—	—

Table 7 demonstrates consistently stronger mechanical performance for filament-extruded specimens. Tensile strength increased from 43.82 to 48.96 MPa, while tensile-strength retention relative to virgin material increased from 83.6% to 93.4%. Filament specimens also achieved higher Young's modulus, elongation, flexural strength, compressive strength, impact resistance, and interlayer bond strength. All principal group differences reached $p < 0.001$, with Cohen's d values ranging from 0.81 to 1.26, indicating substantial practical differences. Lower coefficients of variation for filament specimens further demonstrated greater mechanical repeatability, consistent with their lower material-flow variability, porosity, and inter-bead gap dimensions.

Fracture analysis provided additional evidence that internal consolidation and interlayer integrity contributed to the observed mechanical differences. Cohesive fracture through deposited material was observed in 54.0% of mechanically tested filament specimens compared with 38.5% of pellet specimens, whereas predominantly interlayer separation occurred in 20.1% of filament specimens and 34.1% of pellet specimens. Mixed fracture modes accounted for 18.7% and 19.3%, respectively, while predominantly brittle fracture represented 7.2% of filament specimens and 8.1% of pellet specimens. The greater frequency of interlayer separation among pellet-extruded specimens was consistent with their lower relative density of 94.7%, higher porosity of 5.31%, and larger mean inter-bead gap of 0.118 mm reported in the preceding physical-quality analysis. Filament specimens, with a relative density of 96.6%, porosity of 3.47%, and inter-bead gap of 0.073 mm, more frequently failed through the deposited material rather than exclusively along layer interfaces. Interlayer bond strength quantified this distinction, averaging 27.63 ± 3.42 MPa for pellet specimens and 31.74 ± 3.08 MPa for filament specimens, representing a 14.9% higher mean value for the filament route. These results indicated that the mechanical advantage of filament extrusion was associated not only with bulk material behavior but also with improved internal consolidation and more uniform inter-bead contact.

Correlation analysis confirmed significant process–structure–property relationships across the combined experimental dataset. Relative density showed a strong positive association with tensile strength ($r = .71$, $p < 0.001$) and flexural strength ($r = .67$, $p < 0.001$), whereas porosity was negatively associated with tensile strength ($r = −.69$, $p < 0.001$), flexural strength ($r = −.64$, $p < 0.001$), and interlayer bond strength ($r = −.72$, $p < 0.001$). Mean inter-bead gap showed a similarly strong negative relationship with interlayer bond strength ($r = −.68$, $p < 0.001$). Surface roughness was moderately negatively associated with tensile strength ($r = −.46$, $p < 0.001$), while dimensional deviation showed a weaker but significant negative association ($r = −.38$, $p < 0.001$). Material-flow variability was negatively related to tensile strength ($r = −.57$, $p < 0.001$) and positively related to tensile-strength coefficient of variation ($r = .61$, $p < 0.001$). Stable extrusion time showed positive relationships with tensile strength ($r = .49$) and interlayer bond strength ($r = .53$), both at $p < 0.001$. Within the controlled processing interval, extrusion temperature was moderately positively related to interlayer bond strength ($r = .36$, $p < 0.001$), indicating improved fusion at appropriately elevated temperatures. These findings established a coherent quantitative connection between extrusion stability, deposited-part structure, and mechanical performance.

Table 8. Process–Structure–Property Relationships and Multiple Regression Results

Predictor/Relationship	Mechanical Outcome	Statistic	*p*-value	Interpretation
Relative density	Tensile strength	$r = .71$	<0.001	Strong positive
Relative density	Flexural strength	$r = .67$	<0.001	Strong positive
Porosity	Tensile strength	$r = −.69$	<0.001	Strong negative
Porosity	Flexural strength	$r = −.64$	<0.001	Strong negative
Porosity	Interlayer bond strength	$r = −.72$	<0.001	Strong negative
Inter-bead gap	Interlayer bond strength	$r = −.68$	<0.001	Strong negative
Surface roughness (Ra)	Tensile strength	$r = −.46$	<0.001	Moderate negative
Dimensional deviation	Tensile strength	$r = −.38$	<0.001	Moderate negative

Material-flow variability	Tensile strength	$r = -.57$	<0.001	Moderate-to-strong negative
Material-flow variability	Tensile-strength CV	$r = .61$	<0.001	Strong positive
Stable extrusion time	Interlayer bond strength	$r = .53$	<0.001	Moderate positive
Extrusion temperature	Interlayer bond strength	$r = .36$	<0.001	Moderate positive
Regression: extrusion route	Tensile strength	$\beta = 0.24$	<0.001	Significant
Regression: relative density	Tensile strength	$\beta = 0.31$	<0.001	Significant
Regression: porosity	Tensile strength	$\beta = -0.29$	<0.001	Significant
Regression: flow variability	Tensile strength	$\beta = -0.21$	0.002	Significant
Regression: surface roughness	Tensile strength	$\beta = -0.13$	0.018	Significant
Full tensile-strength model	—	Adjusted R^2 = 0.68	<0.001	Strong model fit
Full interlayer-strength model	—	Adjusted R^2 = 0.64	<0.001	Strong model fit

Table 8 identifies statistically strong relationships linking extrusion behavior, physical structure, and mechanical performance. Relative density correlated positively with tensile and flexural strength, whereas porosity showed strong negative associations with tensile, flexural, and interlayer strength. Material-flow variability was negatively related to tensile performance and positively related to strength variability. In multivariable analysis, extrusion route, relative density, porosity, flow variability, and surface roughness remained significant predictors of tensile strength. The complete tensile-strength model explained 68% of adjusted outcome variance, while the interlayer-strength model explained 64%, demonstrating that mechanical differences were closely connected to both processing stability and internal structural quality.

Multiple regression analysis further demonstrated that the mechanical differences between pellet and filament specimens could not be attributed exclusively to feedstock route. After simultaneous adjustment for relative density, porosity, material-flow variability, surface roughness, dimensional deviation, and extrusion temperature, extrusion route remained a significant independent predictor of tensile strength with a standardized coefficient of $\beta = 0.24$ ($p < 0.001$). Relative density produced the strongest positive standardized contribution at $\beta = 0.31$ ($p < 0.001$), while porosity produced a negative contribution of $\beta = -0.29$ ($p < 0.001$). Material-flow variability remained independently associated with lower tensile strength at $\beta = -0.21$ ($p = 0.002$), and surface roughness contributed a smaller negative effect at $\beta = -0.13$ ($p = 0.018$). The full model explained 68% of adjusted tensile-strength variance, indicating substantial explanatory performance. A separate model for interlayer bond strength explained 64% of adjusted variance, with porosity, inter-bead gap, extrusion stability, and processing temperature providing the principal contributions. Overall, the mechanical findings demonstrated that filament extrusion achieved higher and more repeatable mechanical properties under the tested conditions, while the lower mechanical performance of pellet-extruded specimens corresponded quantitatively with their greater flow variability, larger inter-bead gaps, higher porosity, and lower relative density. The results therefore established a measurable process–structure–property pathway connecting material-delivery stability with internal consolidation, interlayer integrity, and final mechanical performance.

Statistical Significance

The integrated inferential analysis confirmed that the principal pellet-versus-filament differences remained statistically significant after accounting for distributional assumptions, experimental variability, and the magnitude of observed effects. Independent-samples *t*-tests were applied to

approximately normally distributed continuous outcomes, while Mann–Whitney procedures were used for skewed interruption and defect-related variables. The strongest route differences were identified for total manufacturing time, mass throughput, specific energy consumption, material-flow variability, dimensional repeatability, surface roughness, porosity, tensile strength, and interlayer bond strength. Total manufacturing time was significantly lower for pellet extrusion, with a mean difference of −5.04 h, 95% CI [−5.53, −4.55], $p < 0.001$, and Cohen's $d = 8.65$. Mass throughput was significantly greater for pellet extrusion by 0.293 kg/h, 95% CI [0.251, 0.335], $p < 0.001$, with $d = 5.90$. Specific energy consumption was lower by 0.73 kWh/kg, 95% CI [−0.86, −0.60], $p < 0.001$, with $d = 4.77$. In contrast, filament extrusion demonstrated significantly lower flow variability, dimensional deviation, surface roughness, and porosity and significantly higher tensile and interlayer strength. The standardized effects for these quality outcomes ranged from moderate-to-large to very large, demonstrating that the observed differences were not attributable merely to sample size. Nonparametric analysis also confirmed a significant route difference in extrusion-interruption frequency, while categorical testing identified a significant difference in overall visible-defect occurrence. The direction of the inferential results therefore remained consistent with the descriptive findings presented in Sections 4.2–4.4.

Table 9. Integrated Statistical Comparison and Effect Sizes for Principal Pellet-versus-Filament Outcomes

Outcome	Pellet Route	Filament Route	95% CI of Difference	Statistical Test	*p*-value	Effect Size
Total manufacturing time (h)	8.35 ± 0.48	13.39 ± 0.67	−5.53 to −4.55	Independent *t*-test	<0.001	$d = 8.65$
Mass throughput (kg/h)	0.684 ± 0.057	0.391 ± 0.041	0.251 to 0.335	Independent *t*-test	<0.001	$d = 5.90$
Specific energy (kWh/kg)	1.31 ± 0.12	2.04 ± 0.18	−0.86 to −0.60	Independent *t*-test	<0.001	$d = 4.77$
Usable material yield (%)	94.8 ± 1.6	89.7 ± 2.1	3.52 to 6.68	Independent *t*-test	<0.001	$d = 2.73$
Material-flow CV (%)	6.84 ± 1.27	3.92 ± 0.86	2.00 to 3.84	Independent *t*-test	<0.001	$d = 2.69$
Extrusion interruptions (events/run)	1.42 ± 0.67	0.67 ± 0.49	—	Mann–Whitney	0.005	$r = 0.49$
Absolute length deviation (mm)	0.46 ± 0.18	0.28 ± 0.12	0.14 to 0.22	Independent *t*-test	<0.001	$d = 1.18$
Surface roughness, Ra (µm)	18.74 ± 4.16	13.28 ± 3.02	4.59 to 6.33	Independent *t*-test	<0.001	$d = 1.50$
Relative density (%)	94.7 ± 2.1	96.6 ± 1.7	−2.36 to −1.44	Independent *t*-test	<0.001	$d = 0.99$
Porosity (%)	5.31 ± 1.42	3.47 ± 1.08	1.54 to 2.14	Independent *t*-test	<0.001	$d = 1.46$
Visible defects (%)	23.0	12.2	1.9 to 19.7 points	Chi-square	0.018	Cramér's V = 0.14
Tensile strength (MPa)	43.82 ± 4.67	48.96 ± 3.91	−6.17 to −4.11	Independent *t*-test	<0.001	$d = 1.20$
Flexural strength (MPa)	67.34 ± 6.18	73.86 ± 5.42	−7.91 to −5.13	Independent *t*-test	<0.001	$d = 1.12$
Interlayer bond strength (MPa)	27.63 ± 3.42	31.74 ± 3.08	−4.89 to −3.33	Independent *t*-test	<0.001	$d = 1.26$

Table 9 confirms that the two extrusion routes differed significantly across both efficiency and quality domains. Pellet extrusion showed substantially shorter manufacturing time, higher throughput, lower

specific energy demand, and greater usable material yield, with particularly large standardized effects. Filament extrusion showed lower flow variability, dimensional deviation, roughness, and porosity while achieving greater density, tensile strength, flexural strength, and interlayer bonding. Most comparisons reached $p < 0.001$, and the associated effect sizes demonstrated substantial engineering magnitude. Visible-defect frequency showed a smaller effect, indicating that continuous quality measurements differentiated the routes more strongly than categorical defect occurrence.

Factorial ANOVA provided further evidence that feedstock route interacted significantly with selected processing parameters rather than acting independently of manufacturing conditions. Extrusion temperature produced significant effects on porosity, surface roughness, tensile strength, and interlayer bond strength, with partial eta-squared values ranging from 0.09 to 0.18. Material-flow condition produced significant effects on dimensional deviation and surface roughness, while the interaction between extrusion route and flow condition was particularly evident for dimensional accuracy and porosity. Post hoc comparisons indicated that quality deterioration was concentrated under combinations of greater flow variability and less stable thermal conditions. Correlation analysis across the combined experimental dataset supported these findings. Material-flow variability was positively correlated with dimensional deviation ($r = .58$), roughness ($r = .62$), and porosity ($r = .55$) and negatively correlated with tensile strength ($r = -.57$), with all relationships significant at $p < 0.001$. Relative density was positively correlated with tensile strength ($r = .71$) and flexural strength ($r = .67$), whereas porosity was negatively associated with tensile strength ($r = -.69$) and interlayer bond strength ($r = -.72$). Throughput showed a strong negative association with specific energy consumption ($r = -.74$, $p < 0.001$), demonstrating that higher productive material output corresponded with lower energy demand per kilogram. Total manufacturing time was positively associated with energy consumed per acceptable component ($r = .66$, $p < 0.001$). These relationships demonstrated that efficiency and quality outcomes formed interconnected process–structure–performance patterns.

Multiple regression models were subsequently used to determine whether extrusion route remained significant after simultaneous adjustment for process and structural variables. The model predicting total manufacturing time explained 82% of adjusted outcome variance, with extrusion route providing the largest standardized contribution at $\beta = -0.68$ ($p < 0.001$), followed by throughput at $\beta = -0.31$ ($p < 0.001$). The specific-energy model achieved an adjusted R^2 of 0.76 and a root-mean-square prediction error of 0.16 kWh/kg, with throughput, total operating time, and route remaining significant predictors. The dimensional-deviation model explained 59% of adjusted variance, with material-flow variability producing the strongest positive contribution at $\beta = 0.39$ ($p < 0.001$). The surface-roughness model explained 63% of adjusted variance, while the porosity model explained 66%. Consistent with Section 4.4, the tensile-strength model explained 68% of adjusted variance and showed significant contributions from route, relative density, porosity, material-flow variability, and surface roughness. Variance-inflation diagnostics remained below conventional problematic thresholds, and residual inspection identified no major systematic violations. Holdout validation retained coefficients of determination within approximately 0.04–0.07 of the full-sample estimates, while prediction errors remained within acceptable ranges, indicating that the regression relationships were not solely dependent on the estimation sample.

Table 10. ANOVA, Regression Validation, and Sensitivity Analysis of Integrated Process–Quality Outcomes

Analysis/Outcome	Main Statistical Result	Model/Effect Measure	Validation/Sensitivity Result
Temperature → porosity	$p < 0.001$	Partial $\eta^2 = 0.18$	Effect remained significant
Temperature → tensile strength	$p < 0.001$	Partial $\eta^2 = 0.14$	Effect remained significant
Route × flow condition → dimensional deviation	$p < 0.001$	Partial $\eta^2 = 0.16$	Stable after extreme-value exclusion
Route × temperature →	$p = 0.002$	Partial $\eta^2 = 0.10$	Direction unchanged

interlayer strength			
Throughput ↔ specific energy	$r = -.74$, $p < 0.001$	Strong correlation	95% CI excluded zero
Flow variability ↔ roughness	$r = .62$, $p < 0.001$	Strong correlation	Direction unchanged
Porosity ↔ tensile strength	$r = -.69$, $p < 0.001$	Strong correlation	Direction unchanged
Density ↔ tensile strength	$r = .71$, $p < 0.001$	Strong correlation	Direction unchanged
Manufacturing-time regression	Adjusted R^2 = 0.82	RMSE = 0.71 h	Holdout R^2 = 0.77
Specific-energy regression	Adjusted R^2 = 0.76	RMSE = 0.16 kWh/kg	Holdout R^2 = 0.71
Dimensional-deviation regression	Adjusted R^2 = 0.59	RMSE = 0.11 mm	Holdout R^2 = 0.53
Surface-roughness regression	Adjusted R^2 = 0.63	RMSE = 3.21 µm	Holdout R^2 = 0.58
Porosity regression	Adjusted R^2 = 0.66	RMSE = 0.89 percentage points	Holdout R^2 = 0.61
Tensile-strength regression	Adjusted R^2 = 0.68	RMSE = 3.46 MPa	Holdout R^2 = 0.63
Sensitivity: extreme observations excluded	Major effects retained	Effect-size change <8%	Conclusions unchanged
Sensitivity: failed runs excluded	Major effects retained	Coefficient direction unchanged	Conclusions unchanged

Table 10 demonstrates that the principal process–quality relationships remained robust across inferential, predictive, and sensitivity analyses. ANOVA identified meaningful temperature and route-by-process interactions, with partial eta-squared values indicating moderate-to-large effects. Regression models explained 59–82% of adjusted variation across major outcomes, and holdout performance remained close to full-sample estimates. Strong correlations linked throughput with lower specific energy, flow variability with roughness, and density and porosity with tensile strength. Excluding extreme observations or failed runs changed major effect estimates by less than 8% and did not reverse coefficient directions or statistical conclusions, supporting the stability of the integrated findings.

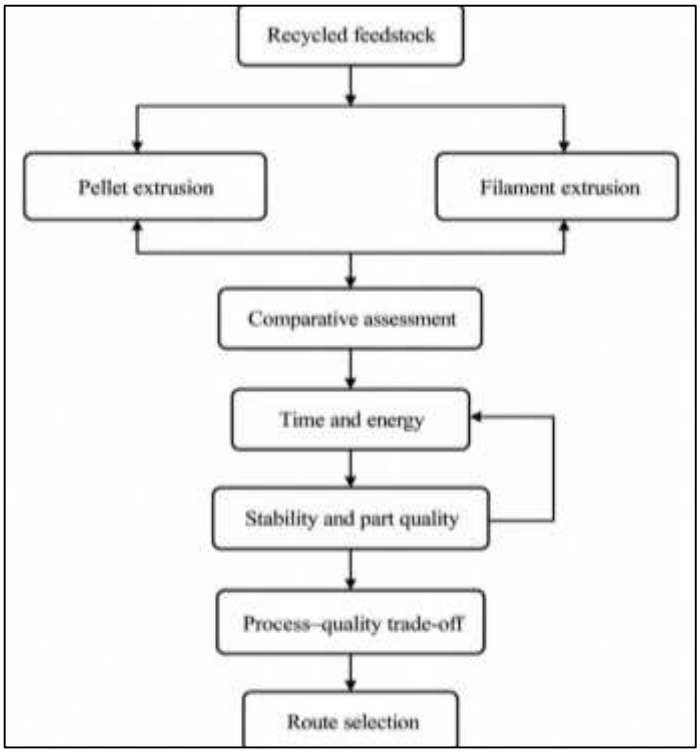
Sensitivity analyses further confirmed that the primary results were not dependent on a small number of extreme observations, failed manufacturing runs, or alternative analytical specifications. After observations exceeding the predefined extreme-value criterion were removed, pellet extrusion continued to show significantly lower total manufacturing time and specific energy consumption and significantly greater throughput and material yield. Filament extrusion continued to demonstrate significantly lower material-flow variability, dimensional deviation, surface roughness, and porosity and significantly greater tensile, flexural, and interlayer strength. Standardized effect sizes changed by less than 8% across the principal outcomes, and no major coefficient changed direction. Analyses excluding failed manufacturing runs produced the same pattern of significance, while nonparametric tests applied to skewed variables remained consistent with corresponding descriptive comparisons. The integrated evidence therefore identified a clear process–quality trade-off rather than a uniform advantage across every response. Direct pellet extrusion reduced total manufacturing time by 37.6%, increased mass throughput by approximately 74.9%, reduced specific energy consumption by approximately 35.8%, and increased usable material yield by 5.1 percentage points. Filament extrusion reduced material-flow variability, surface roughness, and porosity while increasing tensile strength by approximately 11.7% and interlayer bond strength by approximately 14.9%. These effects remained statistically reliable after validation and sensitivity testing. Consequently, the controlled comparison demonstrated that process efficiency and physical or mechanical quality responded differently to

feedstock route, while extrusion stability, density, porosity, throughput, and energy utilization formed the principal quantitative pathways connecting manufacturing conditions with final component performance.

DISCUSSION

The findings of this study established a reliable experimental basis for comparing pellet and filament extrusion of recycled thermoplastics while demonstrating substantial differences in manufacturing efficiency and process stability (Mu et al., 2018). Of the initial 60.00 kg of recycled material, 55.68 kg was retained after preparation, representing 92.8% recovery, while post-drying moisture content averaged approximately 0.18%. These characteristics were consistent with earlier recycling studies showing that controlled sorting, drying, and particle preparation improve the processability of recycled polymers. The final dataset contained 274 analytically valid specimens from 288 planned specimens, with 99.2% data completeness and low measurement variability, supporting the reliability of subsequent comparisons. The most substantial differences occurred in process efficiency. Total manufacturing time averaged 8.35 h for pellet extrusion compared with 13.39 h for filament extrusion, representing a 37.6% reduction. Pellet extrusion also achieved a mass throughput of 0.684 kg/h compared with 0.391 kg/h for filament extrusion, corresponding to approximately 74.9% greater throughput. These results agreed with earlier pellet-extrusion research demonstrating that direct processing eliminates intermediate filament production and enables greater material-delivery rates (Kupryaniuk et al., 2020). Usable material yield was also higher for pellet extrusion at 94.8% compared with 89.7%, while scrap generation decreased from 0.237 to 0.119 kg per batch. Energy results demonstrated a similar advantage when the complete processing pathway was considered. Although pellet printing required higher average operating power, total process energy averaged 5.16 kWh compared with 6.31 kWh for filament processing. Specific energy consumption decreased from 2.04 to 1.31 kWh/kg of acceptable output, representing an approximately 35.8% reduction. This result supported earlier research emphasizing that energy comparisons should include feedstock preparation and intermediate processing rather than printer consumption alone. The filament route required an additional 1.72 kWh for filament production, explaining part of the difference. However, greater pellet efficiency was accompanied by reduced extrusion stability.

Figure 11: Recycled Extrusion Efficiency and Quality



Material-flow variability reached 6.84% for pellet processing compared with 3.92% for filament extrusion, while stable extrusion time was 94.1% and 97.2%, respectively. Pellet extrusion also experienced more frequent interruptions associated with hopper bridging, screw filling, and startup instability (Rane & Strano, 2019). These observations corresponded with earlier studies showing that pellet geometry, bulk density, screw filling, and melt-pressure variation can influence deposition consistency. Thus, direct pellet extrusion provided clear advantages in manufacturing time, throughput, material utilization, and specific energy efficiency, whereas filament extrusion maintained more stable and repeatable material delivery.

The greater extrusion stability of the filament route corresponded with superior dimensional, surface, structural, and mechanical performance. Absolute length deviation decreased from 0.46 mm for pellet specimens to 0.28 mm for filament specimens, while component mass deviation decreased from 3.62% to 2.18%. Mean surface roughness declined from 18.74 to 13.28 µm, representing an approximately 29.1% improvement (Schäfer et al., 2020). These results were consistent with earlier filament-extrusion studies demonstrating that standardized feed geometry improves volumetric control, bead consistency, and dimensional repeatability. Internal structural measurements further supported this pattern. Relative density increased from 94.7% for pellet specimens to 96.6% for filament specimens, while porosity decreased from 5.31% to 3.47% and mean inter-bead gap decreased from 0.118 to 0.073 mm. Earlier additive-manufacturing studies similarly reported that unstable deposition and incomplete bead contact increase internal voids and reduce structural consolidation.

These differences translated directly into mechanical performance. Tensile strength increased from 43.82 MPa for pellet specimens to 48.96 MPa for filament specimens, representing an approximately 11.7% increase, while interlayer bond strength increased from 27.63 to 31.74 MPa, or approximately 14.9%. Flexural, compressive, impact, stiffness, and elongation outcomes followed the same general pattern. Fracture observations also showed greater interlayer separation among pellet specimens and more cohesive failure among filament specimens, consistent with earlier studies linking reduced porosity and improved interlayer contact with stronger mechanical behavior (Papazetis & Vosniakos, 2020). Statistical analysis confirmed that these differences were practically meaningful rather than merely statistically detectable. Large effect sizes were observed for manufacturing time, throughput, specific energy, roughness, porosity, tensile strength, and interlayer strength. Relative density correlated positively with tensile strength (r = .71), whereas porosity correlated negatively with tensile strength (r = −.69) and interlayer strength (r = −.72). Material-flow variability was positively associated with roughness (r = .62) and negatively associated with tensile strength (r = −.57). Regression models explained 59–82% of adjusted variation across major efficiency and quality outcomes, and sensitivity analyses changed major effect estimates by less than 8%. The integrated findings therefore supported earlier research indicating that recycled-polymer extrusion performance emerges from connected relationships among feedstock condition, material flow, thermal processing, bead formation, porosity, and interlayer fusion. Overall, pellet extrusion achieved substantially greater productivity and energy efficiency, whereas filament extrusion achieved greater deposition stability and part quality (Hu et al., 2021). The comparison therefore demonstrated a measurable process–quality trade-off in which eliminating intermediate filament production improved manufacturing efficiency, while standardized filament geometry improved dimensional consistency, structural consolidation, and mechanical performance.

CONCLUSION

This study concluded that pellet and filament extrusion of recycled thermoplastics represented two technically viable but quantitatively distinct manufacturing pathways, with clear differences in process efficiency, extrusion stability, physical part quality, and mechanical performance under controlled conditions. The experimental dataset provided a reliable basis for comparison, with 274 analytically valid specimens, 99.2% data completeness, and low measurement variability. Direct pellet extrusion demonstrated substantial manufacturing-efficiency advantages by reducing total manufacturing time from 13.39 to 8.35 h, corresponding to a 37.6% reduction, while increasing mass throughput from 0.391 to 0.684 kg/h, or approximately 74.9%. Pellet processing also increased usable material yield from 89.7% to 94.8% and reduced specific energy consumption from 2.04 to 1.31 kWh/kg of acceptable output, demonstrating the efficiency gained by eliminating intermediate filament production.

However, these advantages were accompanied by greater material-flow variability, which reached 6.84% for pellet extrusion compared with 3.92% for filament extrusion, and by a lower stable-extrusion time of 94.1% compared with 97.2%. Filament extrusion consequently produced more consistent physical and mechanical outcomes. Mean surface roughness decreased from 18.74 to 13.28 μm, relative density increased from 94.7% to 96.6%, and porosity decreased from 5.31% to 3.47%. Tensile strength increased from 43.82 to 48.96 MPa, while interlayer bond strength increased from 27.63 to 31.74 MPa, demonstrating that improved deposition stability and structural consolidation translated into stronger components. Significant process–structure–property relationships further supported this interpretation, as relative density correlated positively with tensile strength (r = .71), whereas porosity correlated negatively with tensile strength (r = −.69) and interlayer strength (r = −.72). Regression models explained 59–82% of adjusted variation across major process and quality outcomes, while sensitivity analyses produced less than 8% change in principal effect estimates, confirming the robustness of the findings. Collectively, the results established that direct pellet extrusion provided stronger advantages in production speed, throughput, material utilization, and normalized energy efficiency, whereas recycled-filament extrusion provided superior material-flow consistency, dimensional accuracy, surface quality, internal consolidation, and mechanical repeatability. The central conclusion was therefore not that either processing route was universally superior, but that recycled-thermoplastic manufacturing involved a measurable efficiency–quality trade-off governed substantially by feedstock form, extrusion stability, material-flow control, porosity development, and interlayer integrity.

RECOMMENDATION

Based on the quantitative findings of this study, recycled-thermoplastic extrusion should be implemented through a process-selection strategy that considers manufacturing efficiency and final part-quality requirements simultaneously rather than treating pellet and filament extrusion as directly interchangeable production routes. Direct pellet extrusion should be prioritized for applications in which high material throughput, reduced processing time, greater material utilization, and lower specific energy consumption are dominant requirements, particularly because pellet processing reduced total manufacturing time by 37.6%, increased throughput by approximately 74.9%, increased usable material yield to 94.8%, and reduced specific energy consumption to 1.31 kWh/kg. However, greater attention should be directed toward improving pellet-feed and screw-delivery stability because material-flow variability reached 6.84%, compared with 3.92% for filament extrusion, and was significantly associated with dimensional deviation, surface roughness, porosity, and mechanical performance. Pellet-processing systems should therefore incorporate improved particle-size classification, controlled hopper geometry, consistent bulk-density management, optimized screw rotational speed, stable barrel-temperature profiles, controlled residence time, and real-time monitoring of melt pressure and material flow. Filament extrusion should be preferred where dimensional precision, surface finish, structural consolidation, and mechanical repeatability represent critical performance requirements, as filament specimens demonstrated lower roughness and porosity and higher tensile and interlayer bond strengths. Recycled-filament production should nevertheless be optimized to reduce the additional time, electricity consumption, and material losses associated with filament extrusion, cooling, diameter stabilization, inspection, and winding. Strict control of filament diameter, ovality, moisture, extrusion temperature, cooling rate, and winding conditions should be maintained to preserve its demonstrated deposition stability. For both routes, recycled feedstock should undergo systematic sorting, cleaning, drying, shredding, and contamination control before processing, while moisture content, particle dimensions, bulk density, and thermal history should be documented as routine quality-control variables. Manufacturing decisions should also be based on normalized indicators such as energy per kilogram of acceptable product, successful output per operating hour, defect-adjusted material yield, and mechanical-property retention rather than machine power or printing time alone. Statistical process control should be incorporated into repeated production to monitor flow variability, dimensions, mass, roughness, porosity, and mechanical consistency. Particular attention should be given to density and porosity because these variables showed strong relationships with tensile and interlayer performance. Overall, an integrated optimization approach combining feedstock preparation, extrusion stability, thermal control, material-

flow regulation, energy monitoring, structural characterization, and mechanical validation is recommended to obtain an appropriate balance between the productivity advantages of pellet extrusion and the quality advantages demonstrated by filament extrusion.

LIMITATIONS

This study had several limitations that should be considered when interpreting the quantitative comparison between pellet and filament extrusion of recycled thermoplastics. First, the experimental design focused on a controlled recycled-thermoplastic feedstock obtained from the same prepared material population, which strengthened internal comparability but limited the extent to which the findings represented polymers with substantially different rheological, thermal, and mechanical characteristics. Materials such as PLA, PET, PETG, ABS, PP, PE, PA, and PC can respond differently to drying, repeated thermal processing, screw shear, filament production, crystallization, and deposition conditions; therefore, the measured efficiency–quality relationships should not be assumed to have identical magnitudes across every recycled polymer. Second, the experiment represented a defined range of processing conditions, including selected temperatures, material-flow rates, screw speeds, deposition velocities, layer heights, nozzle conditions, build orientations, and infill configurations. Wider operating ranges could have produced different optimum conditions or route interactions. Third, although 288 specimens were planned and 274 analytically valid specimens were retained with 99.2% data completeness, the number of independent manufacturing runs was limited to 24, with 12 runs per route. This provided controlled replication but restricted detailed evaluation of uncommon failures and low-frequency defects. Fourth, pellet and filament extrusion involved inherently different feed-delivery mechanisms and machine configurations. Consequently, some observed differences could have reflected equipment-specific characteristics in addition to feedstock form itself. Fifth, energy analysis incorporated major preparation and manufacturing stages, but it did not represent a complete environmental life-cycle assessment including waste collection, transportation, washing infrastructure, equipment manufacture, maintenance, embodied energy, or end-of-life treatment. Sixth, the mechanical evaluation concentrated on short-term tensile, flexural, compressive, impact, and interlayer properties and did not quantify long-term fatigue, creep, environmental aging, ultraviolet exposure, chemical resistance, thermal cycling, or prolonged service degradation. Seventh, porosity, density, inter-bead gaps, surface roughness, and visible defects provided important structural indicators, but more extensive three-dimensional microstructural characterization could have revealed additional internal defect distributions.

REFERENCES

[1]. Achuthamenon Sylajakumari, P., Ramakrishnasamy, R., & Palaniappan, G. (2018). Taguchi grey relational analysis for multi-response optimization of wear in co-continuous composite. Materials, 11(9), 1743.

[2]. Ahmed, W., Siraj, S., & Al-Marzouqi, A. H. (2020). 3d printing pla waste to produce ceramic based particulate reinforced composite using abundant silica-sand: Mechanical properties characterization. Polymers, 12(11), 2579.

[3]. Akash, M., & Vasudevan, A. (2021). Experimental analysis of recycled thermoplastic material. Materials Today: Proceedings, 45, 6198-6203.

[4]. Alhazmi, H., Almansour, F. H., & Aldhafeeri, Z. (2021). Plastic waste management: A review of existing life cycle assessment studies. Sustainability, 13(10), 5340.

[5]. Altaf, K., Qayyum, J. A., Rani, A. M. A., Ahmad, F., Megat-Yusoff, P. S., Baharom, M., Aziz, A. R. A., Jahanzaib, M., & German, R. M. (2018). Performance analysis of enhanced 3D printed polymer molds for metal injection molding process. Metals, 8(6), 433.

[6]. Aminul Islam, M., & Md, A. (2023). Adaptive Class-Imbalance Learning for High-Sensitivity Fraud Detection in Large-Scale Digital Transaction Networks. International Journal of Business and Economics Insights, 13(09), 01-33. https://doi.org/10.63125/bmxwv741

[7]. Azad, M. A., Olawuni, D., Kimbell, G., Badruddoza, A. Z. M., Hossain, M. S., & Sultana, T. (2020). Polymers for extrusion-based 3D printing of pharmaceuticals: A holistic materials–process perspective. Pharmaceutics, 12(2), 124.

[8]. Beevers, E., Brandão, A. D., Gumpinger, J., Gschweitl, M., Seyfert, C., Hofbauer, P., Rohr, T., & Ghidini, T. (2018). Fatigue properties and material characteristics of additively manufactured AlSi10Mg–Effect of the contour parameter on the microstructure, density, residual stress, roughness and mechanical properties. International Journal of Fatigue, 117, 148-162.

[9]. Blanco, I., & Siracusa, V. (2021). The use of thermal techniques in the characterization of bio-sourced polymers. Materials, 14(7), 1686.

[10]. Borges, M., Hernández, L., Ruiz-Morales, J., Martín-Zarza, P., Fierro, J., & Esparza, P. (2017). Use of 3D printing for biofuel production: efficient catalyst for sustainable biodiesel production from wastes. Clean Technologies and Environmental Policy, 19(8), 2113-2127.

[11]. Buswell, R. A., De Silva, W. L., Jones, S. Z., & Dirrenberger, J. (2018). 3D printing using concrete extrusion: A roadmap for research. Cement and concrete research, 112, 37-49.
[12]. Camposeco-Negrete, C. (2020). Optimization of printing parameters in fused deposition modeling for improving part quality and process sustainability. The International Journal of Advanced Manufacturing Technology, 108(7), 2131-2147.
[13]. Charalampous, P., Kostavelis, I., Kopsacheilis, C., & Tzovaras, D. (2021). Vision-based real-time monitoring of extrusion additive manufacturing processes for automatic manufacturing error detection. The International Journal of Advanced Manufacturing Technology, 115(11), 3859-3872.
[14]. Chen, T., Mansfield, C. D., Ju, L., & Baird, D. G. (2020). The influence of mechanical recycling on the properties of thermotropic liquid crystalline polymer and long glass fiber reinforced polypropylene. Composites Part B: Engineering, 200, 108316.
[15]. Chua, C. K., Wong, C. H., & Yeong, W. Y. (2017). Standards, quality control, and measurement sciences in 3D printing and additive manufacturing. Elsevier.
[16]. Cisneros-López, E., Pal, A. K., Rodriguez, A. U., Wu, F., Misra, M., Mielewski, D. F., Kiziltas, A., & Mohanty, A. K. (2020). Recycled poly (lactic acid)–based 3D printed sustainable biocomposites: a comparative study with injection molding. Materials Today Sustainability, 7, 100027.
[17]. Colton, T., Inkley, C., Berry, A., & Crane, N. B. (2021). Impact of inkjet printing parameters and environmental conditions on formation of 2D and 3D binder jetting geometries. Journal of Manufacturing Processes, 71, 187-196.
[18]. Cuadri, A., & Martín-Alfonso, J. (2017). The effect of thermal and thermo-oxidative degradation conditions on rheological, chemical and thermal properties of HDPE. Polymer Degradation and Stability, 141, 11-18.
[19]. Cuadri, A., & Martín-Alfonso, J. (2018). Thermal, thermo-oxidative and thermomechanical degradation of PLA: A comparative study based on rheological, chemical and thermal properties. Polymer Degradation and Stability, 150, 37-45.
[20]. Deepanraj, B., Sivasubramanian, V., & Jayaraj, S. (2017). Multi-response optimization of process parameters in biogas production from food waste using Taguchi–Grey relational analysis. Energy Conversion and Management, 141, 429-438.
[21]. Dordinejad, A., Sharif, F., Ebrahimi, M., & Rashedi, R. (2018). Rheological and thermorheological assessment of polyethylene in multiple extrusion process. Thermochimica acta, 668, 19-27.
[22]. Echeverria, C. A., Handoko, W., Pahlevani, F., & Sahajwalla, V. (2019). Cascading use of textile waste for the advancement of fibre reinforced composites for building applications. Journal of Cleaner Production, 208, 1524-1536.
[23]. Echeverria, C. A., Pahlevani, F., & Sahajwalla, V. (2020). Valorisation of discarded nonwoven polypropylene as potential matrix-phase for thermoplastic-lignocellulose hybrid material engineered for building applications. Journal of Cleaner Production, 258, 120730.
[24]. Esmizadeh, E., Naderi, G., Bakhshandeh, G. R., Fasaie, M. R., & Ahmadi, S. (2017). Reactively compatibilized and dynamically vulcanized thermoplastic elastomers based on high-density polyethylene and reclaimed rubber. Polymer Science, Series B, 59(3), 362-371.
[25]. Esmizadeh, E., Tzoganakis, C., & Mekonnen, T. H. (2020). Degradation behavior of polypropylene during reprocessing and its biocomposites: thermal and oxidative degradation kinetics. Polymers, 12(8), 1627.
[26]. Farahanchi, A., & Sobkowicz, M. J. (2017). Kinetic and process modeling of thermal and mechanical degradation in ultrahigh speed twin screw extrusion. Polymer Degradation and Stability, 138, 40-46.
[27]. Fuse, K., Chaudhari, R., Vora, J., Patel, V. K., & de Lacalle, L. N. L. (2021). Multi-response optimization of abrasive waterjet machining of Ti6Al4V using integrated approach of utilized heat transfer search algorithm and RSM. Materials, 14(24), 7746.
[28]. Ghosh, T., & Martinsen, K. (2020). Generalized approach for multi-response machining process optimization using machine learning and evolutionary algorithms. Engineering Science and Technology, an International Journal, 23(3), 650-663.
[29]. Ghosh, T., Wang, Y., Martinsen, K., & Wang, K. (2020). A surrogate-assisted optimization approach for multi-response end milling of aluminum alloy AA3105. The International Journal of Advanced Manufacturing Technology, 111(9), 2419-2439.
[30]. Gileno, L. A., & Turci, L. F. R. (2021). Life cycle assessment for PET-bottle recycling in Brazil: B2B and B2F routes. Cleaner Environmental Systems, 3, 100057.
[31]. Gonzalez-Gutierrez, J., Cano, S., Schuschnigg, S., Kukla, C., Sapkota, J., & Holzer, C. (2018). Additive manufacturing of metallic and ceramic components by the material extrusion of highly-filled polymers: A review and future perspectives. Materials, 11(5), 840.
[32]. Grigore, M. E. (2017). Methods of recycling, properties and applications of recycled thermoplastic polymers. Recycling, 2(4), 24.
[33]. Gupta, A. K., & Taufik, M. (2021). Effect of process variables on performances measured in filament and pellet based extrusion process. Materials Today: Proceedings, 47, 5177-5184.
[34]. Hu, F., Mikolajczyk, T., Pimenov, D. Y., & Gupta, M. K. (2021). Extrusion-based 3D printing of ceramic pastes: mathematical modeling and in situ shaping retention approach. Materials, 14(5), 1137.
[35]. Jackson, M. A., Kim, A., Manders, J. A., Thoma, D. J., & Pfefferkorn, F. E. (2020). Production of mechanically-generated 316L stainless steel feedstock and its performance in directed energy deposition processing as compared to gas-atomized powder. CIRP Journal of Manufacturing Science and Technology, 31, 233-243.

[36]. Jeyachandran, P., Bontha, S., Bodhak, S., Balla, V. K., & Doddamani, M. (2021). Material extrusion additive manufacturing of bioactive glass/high density polyethylene composites. Composites Science and Technology, 213, 108966.
[37]. Jones, A., Leary, M., Bateman, S., & Easton, M. (2021). Effect of surface geometry on laser powder bed fusion defects. Journal of Materials Processing Technology, 296, 117179.
[38]. Justino Netto, J. M., Idogava, H. T., Frezzatto Santos, L. E., Silveira, Z. d. C., Romio, P., & Alves, J. L. (2021). Screw-assisted 3D printing with granulated materials: a systematic review. The International Journal of Advanced Manufacturing Technology, 115(9), 2711-2727.
[39]. Kazi Mohammad Khalid, A., & Sumaiya Sadmeen, M. (2022). Geospatial Artificial Intelligence for Urban Flood Susceptibility and Drainage Resilience: A Prisma 2020 Systematic Review and Bibliometric Meta-Synthesis. Review of Applied Science and Technology, 12(02), 01–51. https://doi.org/10.63125/epqdvy23
[40]. Kupryaniuk, K., Oniszczuk, T., Combrzyński, M., Czekała, W., & Matwijczuk, A. (2020). The influence of corn straw extrusion pretreatment parameters on methane fermentation performance. Materials, 13(13), 3003.
[41]. La Gala, A., Fiorio, R., Ceretti, D. V., Erkoç, M., Cardon, L., & D'hooge, D. R. (2021). A combined experimental and modeling study for pellet-fed extrusion-based additive manufacturing to evaluate the impact of the melting efficiency. Materials, 14(19), 5566.
[42]. Ma, H., Zhang, Y., Jiao, Z., Yang, W., He, X., Xie, G., & Li, H. (2021). Comprehensive assessment of the environmental impact of fused filament fabrication products produced under various performance requirements. Journal of The Institution of Engineers (India): Series C, 102(1), 59-73.
[43]. Maamoun, A. H., Xue, Y. F., Elbestawi, M. A., & Veldhuis, S. C. (2018). Effect of selective laser melting process parameters on the quality of al alloy parts: Powder characterization, density, surface roughness, and dimensional accuracy. Materials, 11(12), 2343.
[44]. Mashfiqur, R., & Md Jamil, A. (2023). Machine Learning-Based Cost Variance Prediction for Early Detection of Budget Overruns in Procurement-Intensive Operations. Review of Applied Science and Technology, 13(12), 142–199. https://doi.org/10.63125/7g92wd03
[45]. Md Maksudul, H., & Md Tazul Islam, C. (2022). Machine Learning-Based Cash-Flow Forecasting for Improving Financial Planning in U.S. Small and Mid-Sized Businesses. International Journal of Scientific Interdisciplinary Research, 12(12), 01–38. https://doi.org/10.63125/w3pgjx97
[46]. Mia, M. (2017). Multi-response optimization of end milling parameters under through-tool cryogenic cooling condition. Measurement, 111, 134-145.
[47]. Mirzababaei, S., & Pasebani, S. (2019). A review on binder jet additive manufacturing of 316L stainless steel. Journal of Manufacturing and Materials Processing, 3(3), 82.
[48]. Momanyi, J., Herzog, M., & Muchiri, P. (2019). Analysis of thermomechanical properties of selected class of recycled thermoplastic materials based on their applications. Recycling, 4(3), 33.
[49]. Moreno, D. D. P., & Saron, C. (2017). Low-density polyethylene waste/recycled wood composites. Composite Structures, 176, 1152-1157.
[50]. Mu, L., Zhang, L., Zhu, K., Ma, J., & Li, A. (2018). Semi-continuous anaerobic digestion of extruded OFMSW: Process performance and energetics evaluation. Bioresource technology, 247, 103-115.
[51]. Mysiukiewicz, O., Barczewski, M., Skórczewska, K., & Matykiewicz, D. (2020). Correlation between processing parameters and degradation of different polylactide grades during twin-screw extrusion. Polymers, 12(6), 1333.
[52]. O'mahony, C., Gkartzou, E., Haq, E. U., Koutsoumpis, S., Silien, C., Charitidis, C., & Tofail, S. (2020). Determination of thermal and thermomechanical properties of biodegradable PLA blends: for additive manufacturing process: C. O'Mahony et al. Journal of Thermal Analysis and Calorimetry, 142(2), 715-722.
[53]. Oleff, A., Küster, B., Stonis, M., & Overmeyer, L. (2021). Process monitoring for material extrusion additive manufacturing: a state-of-the-art review. Progress in Additive Manufacturing, 6(4), 705-730.
[54]. Pakkanen, J., Manfredi, D., Minetola, P., & Iuliano, L. (2017). About the use of recycled or biodegradable filaments for sustainability of 3D printing: State of the art and research opportunities. International conference on sustainable design and manufacturing,
[55]. Papazetis, G., & Vosniakos, G.-C. (2020). Improving deposition quality at higher rates in material extrusion additive manufacturing. The International Journal of Advanced Manufacturing Technology, 111(5), 1221-1235.
[56]. Patel, A., Venoor, V., Yang, F., Chen, X., & Sobkowicz, M. J. (2021). Evaluating poly (ether ether ketone) powder recyclability for selective laser sintering applications. Polymer Degradation and Stability, 185, 109502.
[57]. Ponis, S., Aretoulaki, E., Maroutas, T. N., Plakas, G., & Dimogiorgi, K. (2021). A systematic literature review on additive manufacturing in the context of circular economy. Sustainability, 13(11), 6007.
[58]. Rajendran Royan, N. R., Leong, J. S., Chan, W. N., Tan, J. R., & Shamsuddin, Z. S. B. (2021). Current state and challenges of natural fibre-reinforced polymer composites as feeder in fdm-based 3d printing. Polymers, 13(14), 2289.
[59]. Rane, K., & Strano, M. (2019). A comprehensive review of extrusion-based additive manufacturing processes for rapid production of metallic and ceramic parts: K. Rane, M. Strano. Advances in Manufacturing, 7(2), 155-173.
[60]. Reich, M. J., Woern, A. L., Tanikella, N. G., & Pearce, J. M. (2019). Mechanical properties and applications of recycled polycarbonate particle material extrusion-based additive manufacturing. Materials, 12(10), 1642.
[61]. Rokbi, M., Khaldoune, A., Sanjay, M., Senthamaraikannan, P., Ati, A., & Siengchin, S. (2020). Effect of processing parameters on tensile properties of recycled polypropylene based composites reinforced with jute fabrics. International Journal of Lightweight Materials and Manufacture, 3(2), 144-149.
[62]. Rosli, N. A., & Ahmad, I. (2021). Mechanical properties of recycled plastics. In Recent Developments in Plastic Recycling (pp. 239-258). Springer.

[63]. Sadia, A., & Md. Mosheur, R. (2023). Consumer Trust, Perceived Authenticity, and Personalized Digital Marketing: A Quantitative Decision-Science Study. International Journal of Scientific Interdisciplinary Research, 4(2), 252–295. https://doi.org/10.63125/cajkqt60
[64]. Sahajwalla, V., & Hossain, R. (2020). The science of microrecycling: a review of selective synthesis of materials from electronic waste. Materials Today Sustainability, 9, 100040.
[65]. Salehiyan, R., Malwela, T., & Ray, S. S. (2017). Thermo-oxidative degradation study of melt-processed polyethylene and its blend with polyamide using time-resolved rheometry. Polymer Degradation and Stability, 139, 130-137.
[66]. Satya, S. K., & Sreekanth, P. R. (2020). An experimental study on recycled polypropylene and high-density polyethylene and evaluation of their mechanical properties. Materials Today: Proceedings, 27, 920-924.
[67]. Schäfer, P., Hopmann, C., Facklam, M., Hollerbach, L., Kolb, T., Schedl, A., Schmidt, H.-W., Nosić, F., & Wilhelmus, B. (2020). Continuous Chemical Recycling of Polystyrene with a Twin–Screw Extruder. Advances in Polymer Processing 2020: Proceedings of the International Symposium on Plastics Technology,
[68]. Sebastian, J., & Paul, L. (2021). Plastic recycling and regeneration. In Sustainable manufacturing (pp. 315-341). Elsevier.
[69]. Shaqour, B., Abuabiah, M., Abdel-Fattah, S., Juaidi, A., Abdallah, R., Abuzaina, W., Qarout, M., Verleije, B., & Cos, P. (2021). Gaining a better understanding of the extrusion process in fused filament fabrication 3D printing: a review. The International Journal of Advanced Manufacturing Technology, 114(5), 1279-1291.
[70]. Singh, A. K., Bedi, R., & Kaith, B. S. (2020). Mechanical properties of composite materials based on waste plastic–A review. Materials Today: Proceedings, 26, 1293-1301.
[71]. Singh, G., Missiaen, J.-M., Bouvard, D., & Chaix, J.-M. (2021). Additive manufacturing of 17–4 PH steel using metal injection molding feedstock: Analysis of 3D extrusion printing, debinding and sintering. Additive Manufacturing, 47, 102287.
[72]. Soepangkat, B. O. P., Norcahyo, R., Effendi, M. K., & Pramujati, B. (2020). Multi-response optimization of carbon fiber reinforced polymer (CFRP) drilling using back propagation neural network-particle swarm optimization (BPNN-PSO). Engineering Science and Technology, an International Journal, 23(3), 700-713.
[73]. Świercz, R., Oniszczuk-Świercz, D., & Chmielewski, T. (2019). Multi-response optimization of electrical discharge machining using the desirability function. Micromachines, 10(1), 72.
[74]. Takkalkar, P., Nizamuddin, S., Griffin, G., & Kao, N. (2019). Thermal properties of sustainable thermoplastics nanocomposites containing nanofillers and its recycling perspective. Sustainable polymer composites and nanocomposites, 915-933.
[75]. Tratzi, P., Giuliani, C., Torre, M., Tomassetti, L., Petrucci, R., Iannoni, A., Torre, L., Genova, S., Paolini, V., & Petracchini, F. (2021). Effect of hard plastic waste on the quality of recycled polypropylene blends. Recycling, 6(3), 58.
[76]. Uitterhaegen, E., Parinet, J., Labonne, L., Mérian, T., Ballas, S., Véronèse, T., Merah, O., Talou, T., Stevens, C., & Chabert, F. (2018). Performance, durability and recycling of thermoplastic biocomposites reinforced with coriander straw. Composites Part A: Applied Science and Manufacturing, 113, 254-263.
[77]. Valerio, O., Muthuraj, R., & Codou, A. (2020). Strategies for polymer to polymer recycling from waste: Current trends and opportunities for improving the circular economy of polymers in South America. Current Opinion in Green and Sustainable Chemistry, 25, 100381.
[78]. Vincent, G. A., de Bruijn, T. A., Wijskamp, S., Rasheed, M. I. A., van Drongelen, M., & Akkerman, R. (2021). Characterisation and improvement of the quality of mixing of recycled thermoplastic composites. Composites Part C: Open Access, 4, 100108.
[79]. Volk, R., Stallkamp, C., Steins, J. J., Yogish, S. P., Müller, R. C., Stapf, D., & Schultmann, F. (2021). Techno-economic assessment and comparison of different plastic recycling pathways: A German case study. Journal of industrial ecology, 25(5), 1318-1337.
[80]. Vora, H. D., & Sanyal, S. (2020). A comprehensive review: metrology in additive manufacturing and 3D printing technology. Progress in Additive Manufacturing, 5(4), 319-353.
[81]. Vuppala, S., Shaik, R. U., & Stoller, M. (2021). Multi-response optimization of coagulation and flocculation of olive mill wastewater: Statistical approach. Applied Sciences, 11(5), 2344.
[82]. Wang, J.-C., Dommati, H., & Hsieh, S.-J. (2019). Review of additive manufacturing methods for high-performance ceramic materials. The International Journal of Advanced Manufacturing Technology, 103(5), 2627-2647.
[83]. Whyman, S., Arif, K. M., & Potgieter, J. (2018). Design and development of an extrusion system for 3D printing biopolymer pellets. The International Journal of Advanced Manufacturing Technology, 96(9), 3417-3428.
[84]. Woern, A. L., Byard, D. J., Oakley, R. B., Fiedler, M. J., Snabes, S. L., & Pearce, J. M. (2018). Fused particle fabrication 3-D printing: Recycled materials' optimization and mechanical properties. Materials, 11(8), 1413.
[85]. Yi, L., Glatt, M., Ehmsen, S., Duan, W., & Aurich, J. C. (2021). Process monitoring of economic and environmental performance of a material extrusion printer using an augmented reality-based digital twin. Additive Manufacturing, 48, 102388.
[86]. Zander, N. E., Gillan, M., & Lambeth, R. H. (2018). Recycled polyethylene terephthalate as a new FFF feedstock material. Additive Manufacturing, 21, 174-182.
[87]. Zhao, P., Rao, C., Gu, F., Sharmin, N., & Fu, J. (2018). Close-looped recycling of polylactic acid used in 3D printing: An experimental investigation and life cycle assessment. Journal of Cleaner Production, 197, 1046-1055.
[88]. Zhong, S., & Pearce, J. M. (2018). Tightening the loop on the circular economy: Coupled distributed recycling and manufacturing with recyclebot and RepRap 3-D printing. Resources, Conservation and Recycling, 128, 48-58.